



# A Genomic and Bioinformatics View of the Classification and Evolution of *Morganella* Species and Their Chromosomal Accessory Genetic Elements Harboring Antimicrobial Resistance Genes

 Ying Jing,<sup>a</sup> Zhe Yin,<sup>a</sup> Peng Wang,<sup>a</sup> Jiayao Guan,<sup>a</sup> Fangzhou Chen,<sup>a</sup> Lingling Wang,<sup>a</sup> Xinyue Li,<sup>a</sup> Xiaofei Mu,<sup>a</sup>  Dongsheng Zhou<sup>a</sup>

<sup>a</sup>State Key Laboratory of Pathogen and Biosecurity, Beijing Institute of Microbiology and Epidemiology, Beijing, China

Ying Jing and Zhe Yin contributed equally to this article. Author order was determined by the corresponding author after negotiation.

**ABSTRACT** In this study, draft-genome sequencing was conducted for 60 Chinese *Morganella* isolates, and furthermore, 12 of them were fully sequenced. Then, a total of 166 global sequenced *Morganella* isolates, including the above 60, were collected to perform average nucleotide identity-based genomic classification and core single nucleotide polymorphism-based phylogenomic analysis. A genome sequence-based species classification scheme for *Morganella* was established, and accordingly, the two conventional *Morganella* species were redefined as two complexes and further divided into four and two genospecies, respectively. At least 88 acquired antimicrobial resistance genes (ARGs) were disseminated in these 166 isolates and were prevalent mostly in the isolates from hospital settings. IS26/IS15DI, IS10 and IS1R, and Tn3-, Tn21-, and Tn7-subfamily unit transposons were frequently presented in these 166 isolates. Furthermore, a detailed sequence comparison was applied to 18 *Morganella* chromosomal accessory genetic elements (AGEs) from the fully sequenced 12 isolates, together with 5 prototype AGEs from GenBank. These 23 AGEs were divided into eight different groups belonging to composite/unit transposons, transposable prophages, integrative and mobilizable elements, and integrative and conjugative elements, and they harbored at least 52 ARGs involved in resistance to 15 categories of antimicrobials. Eleven of these 23 AGEs acquired large accessory modules, which exhibited complex mosaic structures and contained many antimicrobial resistance loci and associated ARGs. Integration of ARG-containing AGEs into *Morganella* chromosomes would contribute to the accumulation and dissemination of ARGs in *Morganella* and enhance the adaptation and survival of *Morganella* under complex and diverse antimicrobial selection pressures.

**IMPORTANCE** This study presents a comprehensive genomic epidemiology analysis on global sequenced *Morganella* isolates. First, a genome sequence-based species classification scheme for *Morganella* is established with a higher resolution and accuracy than those of the conventional scheme. Second, the prevalence of accessory genetic elements (AGEs) and associated antimicrobial resistance genes (ARGs) among *Morganella* isolates is disclosed based on genome sequences. Finally, a detailed sequence comparison of eight groups of 23 AGEs (including 19 *Morganella* chromosomal AGEs) reveals that *Morganella* chromosomes have evolved to acquire diverse AGEs harboring different profiles of ARGs and that some of these AGEs harbor large accessory modules that exhibit complex mosaic structures and contain a large number of ARGs. Data presented here provide a deeper understanding of the classification and evolution of *Morganella* species and also those of ARG-containing AGEs in *Morganella* at the genomic scale.

**Editor** Tino Polen, Forschungszentrum Jülich GmbH

**Copyright** © 2022 Jing et al. This is an open-access article distributed under the terms of the [Creative Commons Attribution 4.0 International license](https://creativecommons.org/licenses/by/4.0/).

Address correspondence to Dongsheng Zhou, zhouds@bmi.ac.cn and dongshengzhou1977@gmail.com.

The authors declare no conflict of interest.

**Received** 16 December 2021

**Accepted** 1 February 2022

**Published** 23 February 2022

**KEYWORDS** *Morganella*, accessory genetic elements, antimicrobial resistance, genome sequencing, species classification

*Morganella* is ubiquitously present and belongs to the *Morganellaceae* family (1). *Morganella* includes only two described species, *Morganella morganii* and *Morganella psychrotolerans*, based on DNA–DNA hybridization (2), and *M. morganii* is furthermore divided into two subspecies, *morganii* and *sibonii*, according to trehalose fermentation ability (3). The 16S rRNA gene nucleotide similarity between *M. morganii* and *M. psychrotolerans* isolates is 98.6% (2), which is above the threshold of 97% generally used to separate species (4), indicating that these two species cannot be steadily distinguished by 16S rRNA gene sequences.

*M. psychrotolerans* is occasionally isolated from chilled seafood and is recognized as a rainbow trout pathogen (5). *M. morganii* is frequently isolated from hospital settings and represents an important opportunistic pathogen (6). *M. morganii* is naturally resistant to penicillins, the first/second-generation cephalosporins, nitrofurantoin, tigecycline, macrolides, lincosamides, fusidic acid, polymyxins, and glycopeptides (6). *M. morganii* can acquire diverse accessory genetic elements (AGEs), such as unit transposons (7, 8), integrative and conjugative elements (ICEs) (9), and integrative and mobilizable elements (IMEs) (10, 11). These AGEs carry diverse antimicrobial resistance genes (ARGs), such as *bla*<sub>KPC-2</sub> (8), *aadA1* (10), and *qnrD* (12), and thus greatly contribute to the dissemination of antimicrobial resistance in *M. morganii*. Although there are a plenty of reports on identifying AGEs and associated ARGs in *M. morganii*, only few of them are devoted to genetically dissecting their modular structures (7, 10).

This study presented a genomic epidemiology analysis on 166 global sequenced *Morganella* isolates, including 60 sequenced in this study. We established a genome sequence-based species classification scheme for *Morganella* to give a genomic view of *Morganella* species classification and, moreover, disclosed the prevalence of ARG-associated AGEs among *Morganella* isolates. We further performed a detailed sequence comparison of 18 *Morganella* chromosomal AGEs sequenced in this study together with 5 prototype AGEs from GenBank to provide a deeper understanding of *Morganella* AGE diversification.

## RESULTS

**Genomic classification and evolution of *Morganella* species.** We determined the draft-genome sequences of 60 Chinese *Morganella* isolates (Fig. 1 and Table S1) and also the complete genome sequences of 12 of these 60 isolates (see Table S2 for quality control results). We then performed the species classification and phylogenomic analysis on a collection of 166 global sequenced *Morganella* isolates, including the above 60 together with the other 106 from GenBank (last accessed February 1 2021). Based on the conventional scheme for classifying *Morganella* species (2), 161 (96.99%) of them were assigned into *M. morganii* while the remaining 5 (3.01%) were assigned into *M. psychrotolerans*, indicating that the overwhelming majority of *Morganella* isolates belonged to *M. morganii*. Given that the absence and presence of trehalose-utilization operon *treRBP* could be used to distinguish *morganii* and *sibonii* subspecies, respectively (13), it was found here that 147 isolates were assigned into *morganii* subspecies and the remaining 14 were assigned into *sibonii* subspecies (Fig. 2 and Table S1).

To perform genomic classification and phylogeny of *Morganella*, the pairwise average nucleotide identity (ANI) values of these 166 isolates were calculated (Fig. S1 and Table S3). Based on the threshold of 95% ANI for genospecies delineation (14), a total of six genospecies could be classified and then designated *M. morganii*, *M. chanii*, *M. sibonii*, *M. laugraudii*, *M. psychrotolerans*, and *M. kristinii*, respectively. The former four genospecies were assigned into *M. morganii* complex, while the latter two were assigned into *M. psychrotolerans* complex. These two complexes displayed  $\leq 84.4\%$  ANI with each other, while the genospecies within each complex displayed  $\geq 90.5\%$  ANI.

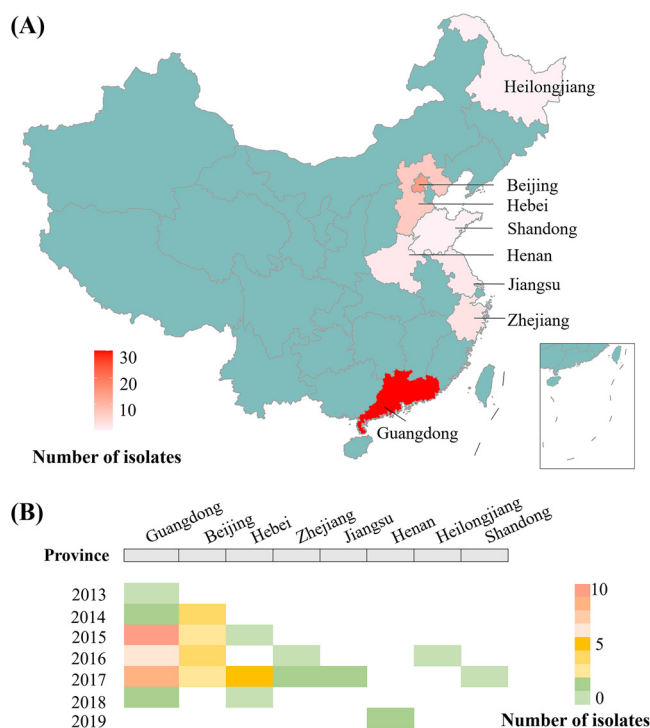


**FIG 1** Spatial-temporal distribution of *Morganella* isolates from China. (A) Distribution of 60 *Morganella* isolates collected in this study in different provinces. (B) Distribution of 60 *Morganella* isolates in different years of different provinces.

The 60 isolates sequenced in this study could be assigned into the two genospecies *M. morganii* ( $n = 59$ ) and *M. sibonii* ( $n = 1$ ) of the *M. morganii* complex.

For further phylogenomic analysis, a total of 3,538 core single nucleotide polymorphisms (SNPs) were identified from these 166 chromosome sequences. The recombination relative to point mutation ( $r/m$ ) value was calculated to evaluate the impact of homologous recombination on sequence diversification (15). An  $r/m$  value of 2.6 was inferred at the genome level, indicating that homologous recombination introduced 2.6 times more nucleotide substitution than point mutation and, thereby, recombination events frequently occurred during genomic evolution and classification of *Morganella* (15). To avoid the influence of homologous recombination on phylogenetic reconstruction, a collection of 1,299 recombination-free SNPs was generated, and a maximum-likelihood phylogenetic tree was constructed using these recombination-free SNPs (Fig. 2). Almost all of the branches in this tree had bootstrap values of  $\geq 70\%$ , suggesting that this recombination-free tree could accurately reflect the evolutionary relatedness and population structure of *Morganella* (16). In this tree, the isolates from *M. morganii* and *M. psychrotolerans* complexes were clustered into two primary phylogroups that split earliest and emerged independently, indicating very distinct evolutionary histories of these two complexes. These two primary phylogroups could be further divided into four and two sub-phylogroups, respectively; as expected, they showed perfect correspondence to the above six genospecies, illustrating the consistency between ANI-based genospecies classification and phylogenomic analysis. The population ( $n = 147$ ) of *M. morganii*, much larger than that of the other five genospecies, exhibited a highly clonal structure independent of geographic locations, time, and specimens of these isolates (Fig. 2 and Table S1).

**Distribution of acquired ARGs among *Morganella* isolates.** At least 88 kinds of acquired ARGs, involved in resistance to 16 different categories of antimicrobials, were identified in these 166 *Morganella* isolates (Fig. S2). All these ARGs were distributed in *M. morganii* complex (116/166, 67.47%), including genospecies *M. morganii* (103/166, 62.04%), *M. sibonii* (10/166, 6.02%), and *M. chanii* (3/166, 1.81%) (Fig. S3 and Table S4).

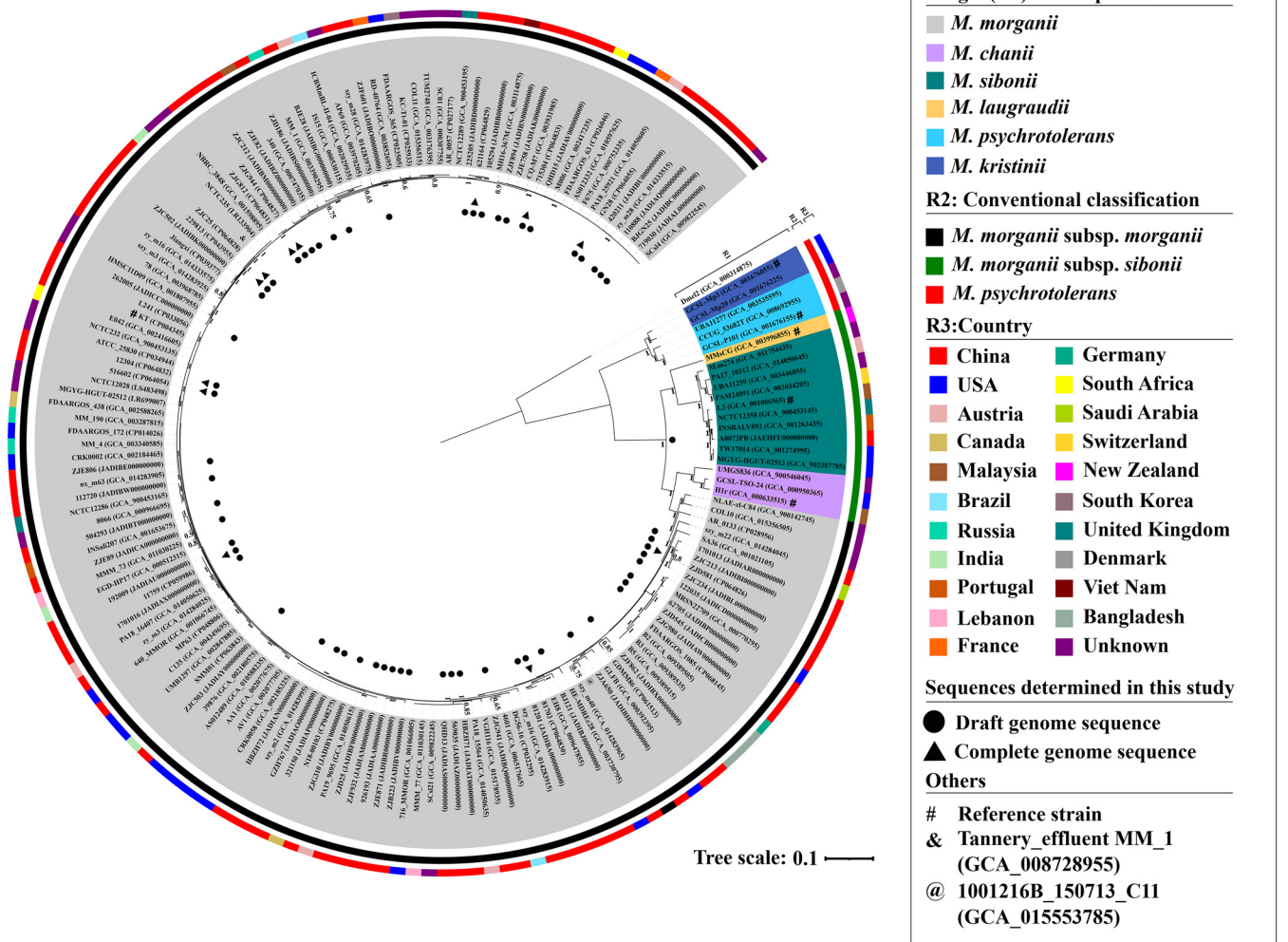


**FIG 2** A maximum-likelihood phylogenetic tree of *Morganella* isolates. Degree of support (percentage) for each cluster of associated taxa, as determined by bootstrap analysis, is shown next to each branch. Bar corresponds to scale of sequence divergence. *Providencia alcalifaciens* isolate Dmel2 (accession number GCA\_000314875) is used as the outgroup. For each genospecies, the isolate is designated the reference if its genome sequence is first uploaded in GenBank. Following the well-established binomial nomenclature principles (52), the genospecies name is designed by using the surname of the person submitting its reference isolate's genome sequence to GenBank.

The most prevalent acquired ARGs were tetracycline-resistance genes (99/166, 59.64%), followed by aminoglycoside-resistance genes (70/166, 42.17%), sulfonamide-resistance genes (62/166, 37.35%), trimethoprim-resistance genes (56/166, 33.73%), and  $\beta$ -lactam-resistance genes (54/166, 32.53%) (Fig. S3 and Table S4).

These 88 acquired ARGs were further assigned into the reservoirs (humans, animals, and the environment) of the 149 isolates with source information (Table S1). *Morganella* isolates from humans contained many more acquired ARGs than those from animals and the environment (Fig. 3A), and moreover, 80 of 88 acquired ARGs (especially including aminoglycoside-resistance genes [ $n = 23, P < 0.0186$ ] and  $\beta$ -lactam-resistance genes [ $n = 15, P < 0.0264$ ]) could be found in human reservoirs (Fig. 3B), indicating that *Morganella* from hospitalized patients had evolved to acquire many more ARGs to encounter complex and high selection of antimicrobials in hospital settings. A total of 18 acquired ARGs, involved in resistance to nine different categories of antimicrobials, were shared by *Morganella* isolates from all the above three reservoirs, denoting a long history of acquisition and wide dissemination of these ARGs in *Morganella*.

Forty-nine of the 60 isolates sequenced here harbored 63 of the above-mentioned 88 ARGs, and these 63 ARGs were involved in resistance to 15 (except for polymyxin) of the above-mentioned 16 antimicrobials (Fig. S2). These 63 ARGs were found in

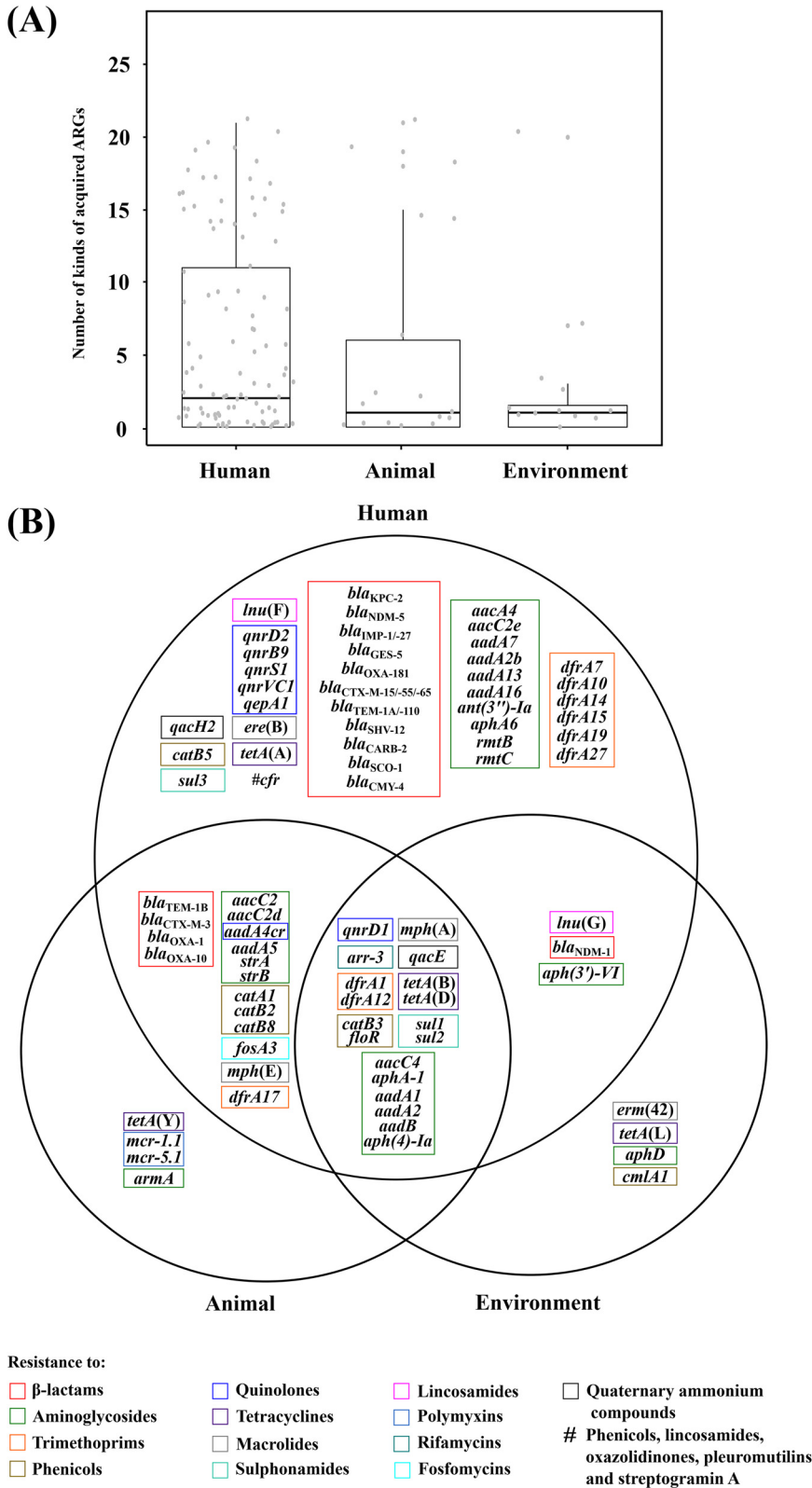


**FIG 3** Distribution of acquired ARGs among *Morganella* isolates. (A) Boxplot displays the number of kinds of acquired ARGs in three reservoirs. (B) Venn diagram shows the distribution of different classes of acquired ARGs in three reservoirs.

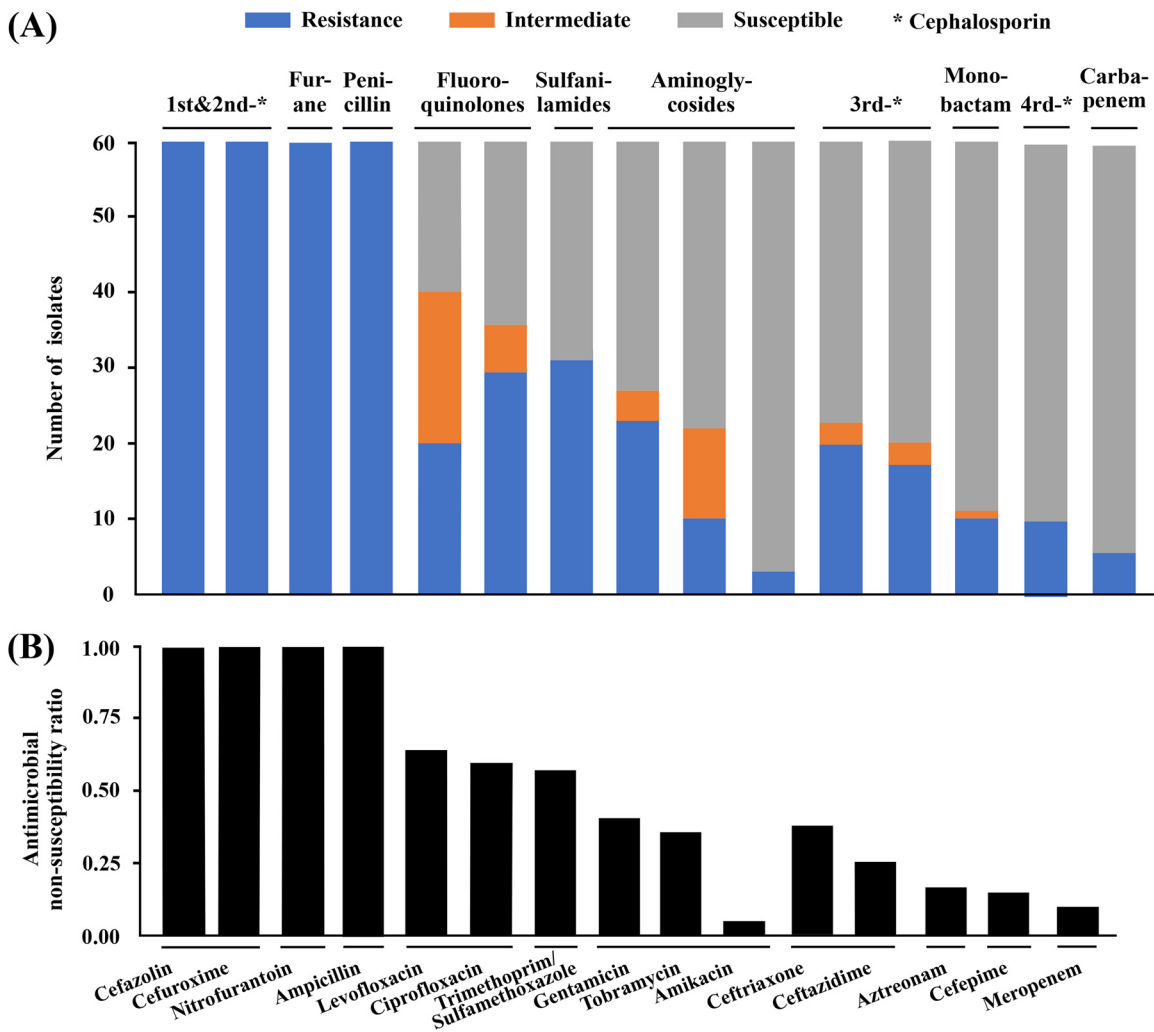


**FIG 4** Antimicrobial susceptibility data of 60 *Morganella* isolates. (A) Shown are the antimicrobial resistance profiles of 60 *Morganella* isolates collected in this study. (B) Shown are the nonsusceptibility rates [(resistant + intermediate)/(sensitivity + intermediate + resistant)] of 60 *Morganella* isolates for each antimicrobial. Original data are shown in Table S1.

genospecies *M. morganii* (48/60, 90%) and *M. sibonii* (1/60, 1.67%). The top 5 ARGs in these 60 isolates were tetracycline-resistance genes (46/60, 81.67%), aminoglycoside-resistance genes (42/60, 70%), sulfonamide-resistance genes (34/60, 56.67%), chloramphenicol-resistance genes (30/60, 50%), and  $\beta$ -lactam-resistance genes (29, 48.33%); this observation was highly similar to the prevalence of 88 acquired ARGs in the 166 isolates described above.

The antimicrobial susceptibility/resistance profiles of these 60 isolates were determined using 15 different antimicrobials (Fig. 4 and Table S1). As expected, all 60 of these isolates were highly resistance to ampicillin, cefazolin, cefuroxime, and nitrofurantoin due to intrinsic resistance. These 60 isolates displayed nonsusceptibility rates of >50% for three antimicrobials, 50% to 20% for four antimicrobials, and <20% for the remaining four antimicrobials, including aztreonam (18.34%, 11/60), cefepime (16.67%, 10/60), meropenem (10%, 6/60), and amikacin (5%, 3/60). *Morganella* isolates in China showed the highest nonsusceptibility rate ( $n = 40$ , 66.67%) for fluoroquinolones, including levofloxacin and ciprofloxacin. Meropenem and amikacin could be the first choice for experiential treatment of *Morganella*-induced infections in China because they have the lowest detected nonsusceptibility rates ( $\leq 10\%$ ). All six of the meropenem-resistance *Morganella* isolates discussed herein acquired the carbapenemase gene *bla*<sub>KPC-2</sub> ( $n = 4$ ) or *bla*<sub>NDM-1</sub>

**TABLE 1** The distribution of 17 major AGE groups in 166 global *Morganella* isolates

Family and subfamily	Core transposition determinant	Genospecies	No. of positive strains	%
<b>IS</b>				
IS26/IS15DI	<i>tnpA</i>	<i>Morganella. morganii</i>	67	41.75
IS26/IS15DI	<i>tnpA</i>	<i>M. sibonii</i>	1	
IS26/IS15DI	<i>tnpA</i>	<i>M. kristinii</i>	1	
IS10	<i>tnpA</i>	<i>M. morganii</i>	65	39.16
IS1R	<i>tnpA</i>	<i>M. morganii</i>	38	23.49
IS1R	<i>tnpA</i>	<i>M. sibonii</i>	1	
<b>Tn3</b>				
Tn3	<i>tnpAR</i>	<i>M. morganii</i>	12	7.23
Tn21	<i>tnpAR</i>	<i>M. morganii</i>	32	19.88
Tn21	<i>tnpAR</i>	<i>M. sibonii</i>	1	
Tn163	<i>tnpAR</i>		0	0
Tn4430	<i>tnpAR</i>		0	0
Tn4651	<i>tnpAR</i>		0	0
Tn4401	<i>tnpAR</i>		0	0
<b>Tn7</b>				
Tn7	<i>tnsABCDE</i>	<i>M. morganii</i>	23	13.86
Tn6230	<i>tnsABCD</i>		0	0
Tn552	<i>tnsCBR</i>		0	0
Tn6022	<i>tnsABCDE</i>		0	0
Tn5053	<i>tniABQR</i>		0	0
<b>Tn554</b>				
Tn554	<i>tnpABC</i>		0	0
Tn6488	<i>ginABCD</i>		0	0
Tn6571	<i>ginABCD</i>		0	0

( $n = 2$ ) (Table S1) and were confirmed to have carbapenemase activity in bacterial cell extracts. There were 25 of these 60 isolates that carried multiple aminoglycoside-modifying enzyme genes and thereby displayed resistance to gentamicin and tobramycin, but only 3 of these 25 isolates were nonsusceptible to amikacin due to the following two reasons: (i) amikacin was insensitive against these enzymes (17) and (ii) these 3 amikacin-resistant isolates additionally acquired the 16S rRNA methyltransferase gene *rmtB*, therefore mediating high-level amikacin resistance (18).

**A global view of AGEs in the 166 sequenced *Morganella* isolates.** AGEs acted as the vectors of ARGs and thus were responsible for the accumulation and dissemination of ARGs in different bacterial isolates by intracellular/intercellular transfer (19). To understand the prevalence of ARG-containing AGEs in *Morganella*, we screened the 166 sequenced *Morganella* isolates for the prevalence of the 17 major AGE groups frequently found in Gram-negative bacteria (Table 1). Detected were 6 of the above 17 groups: IS26/IS15DI, IS10, and IS1R and Tn3-, Tn21-, and Tn7-subfamily unit transposons were found in 69 (41.75%), 65 (39.16%), 39 (23.49%), 12 (7.23%), 33 (19.88%), and 23 (13.86%) of these 166 isolates. These six groups of AGEs were identified in the genospecies *M. morganii* ( $n = 82$ ) and *M. sibonii* ( $n = 3$ ) belonging to *M. morganii* complex and the genospecies *M. kristinii* ( $n = 1$ ) belonging to *M. psychrotolerans* complex. Accordingly, the selection of 12 nonredundant isolates for whole-genome sequencing (see above) was based on the reason that they probably carried at least one of IS26/IS15DI-, IS10-, or IS1R-composite transposons and Tn21- and Tn7-subfamily unit transposons.

**A collection of 23 AGEs for detailed sequence comparison.** Each of these fully sequenced 12 isolates harbored 1 to 3 kinds of chromosomal AGEs, giving a total of 18 identified (Table S5). Additionally, a total of 11 plasmids were identified from 7 of these 12 isolates (see Table S6 for details). Subsequent analysis was then focused on these 18 chromosomal AGEs, further dividing into eight distinct groups: (i) two IS26/IS15DI-composite transposons, Tn6759 and Tn6760 from strains 11759 and 621164, respectively, (ii) three IS10-composite transposons, Tn10, Tn6798, and Tn6799 from strains

**TABLE 2** Major features of AGEs characterized in this study

Group	AGE <sup>a</sup>	Accession no.	Chromosomal nucleotide position	Length (bp)	Host bacterium	Reference
IS26/IS15DI-composite transposons	Tn6759	CP059986	3662767–3668698	5,932	<i>Morganella morganii</i> 11759	This study
	Tn6760	CP064829	2991196–3002147	10,952	<i>M. morganii</i> 621164	This study
Tn10-related elements	Tn10 <sub>ZJC25</sub>	CP064828	1486140–1495286	9,147	<i>M. morganii</i> ZJC25	This study
	Tn10 <sub>229813</sub>	CP043955	1519262–1528408	9,147	<i>M. morganii</i> 229813	This study
	Tn10 <sub>516602</sub>	CP064054	2606745–2615891	9,147	<i>M. morganii</i> 516602	This study
	Tn10 <sub>11759</sub>	CP059986	1720225–1729371	9,147	<i>M. morganii</i> 11759	This study
	Tn6798	CP064829	1802073–1811996	9,924	<i>M. morganii</i> 621164	This study
	Tn6799	CP064833	1990256–1990256	38,672	<i>M. morganii</i> 715304	This study
Tn7-related elements	T10RE <sub>GN28</sub>	CP064055	2305754–2348095	42,342	<i>M. morganii</i> GN28	This study
	Tn7 <sub>ZJC25</sub>	CP064828	19506–33572	14,067	<i>M. morganii</i> ZJC25	This study
	Tn7 <sub>229813</sub>	CP043955	19469–33535	14,067	<i>M. morganii</i> 229813	This study
	Tn6800	CP064830	22578–37741	15,164	<i>M. morganii</i> 81703	This study
Tn1696-related elements	T7RE <sub>621164</sub>	CP064829	20656–62976	42,321	<i>M. morganii</i> 621164	This study
	Tn1696	U12338	Not applicable	16,318	<i>Pseudomonas aeruginosa</i> R1033	23
	Tn6913a	CP064831	1916898–1963812	46,915	<i>M. morganii</i> ZJG812	This study
	Tn6913b	CP064827	2071073–2117588	46,516	<i>M. morganii</i> ZJG944	This study
	Tn6914	CP064828	1968547–1982455	13,909	<i>M. morganii</i> ZJC25	This study
	Tn6915	CP043955	2001667–2051662	49,996	<i>M. morganii</i> 229813	This study
	T1696RE <sub>ZJD581</sub>	CP064826	2049692–2113491	63,800	<i>M. morganii</i> ZJD581	This study
Tn6963-related transposable prophages	Tn6963	CP033056	2191792–2236217	44,426	<i>M. morganii</i> L241	24
Tn6964-related IMEs	Tn6964	CP064832	2277663–2371532	93,870	<i>M. morganii</i> 12304	This study
	Tn6872	LR134189	3025117–3045606	20,490	<i>Providencia rustigianii</i> NCTC6933	Not applicable
Tn6397-related ICES	Tn6966	CP064830	3371703–3442829	71,127	<i>M. morganii</i> 81703	This study
	Tn6397	CP021851	386444–510401	123,958	<i>Enterobacter cloacae</i> A1137	27
Tn2670-related elements	Tn6967	CP064827	628561–738154	109,594	<i>M. morganii</i> ZJG944	This study
	Tn2670	AP000342	Not applicable	22,760	<i>Shigella flexneri</i> R100	28
	T2670RE <sub>11759</sub>	CP059986	2289505–2325366	35,862	<i>M. morganii</i> 11759	This study

<sup>a</sup>T10RE<sub>GN28</sub>, T2670RE<sub>11759</sub>, T7RE<sub>621164</sub> and T1696RE<sub>ZJD581</sub> would lose their intracellular mobility due to the lesion of their core transposition determinants IS10, IS1R, *tnsABCDE*, and *tnpAR*, respectively. The remaining AGEs are intact and would have intracellular or intercellular mobility.

ZJC25/229813/516602/11759, 621164, and 715304, respectively, together with a 43.1-kb Tn10-related element from strain GN28 designated T10RE<sub>GN28</sub> (iii) two Tn7-related unit transposons, Tn7 and Tn6800 from strains 229813 and ZJC25, respectively, together with a 42.3-kb Tn7-related element T7RE<sub>621164</sub> from strain 621164, (iv) four Tn1696-related unit transposons, Tn6913a, Tn6913b, Tn6914, and Tn6915 from strains ZJG812, ZJG944, ZJC25, and 229813, respectively, together with a 63.8-kb Tn1696-related element T1696RE<sub>ZJD581</sub> from strain ZJD581, (v) a Tn6963-related transposable prophage Tn6964 from strain 12304, (vi) a Tn6872-related IME Tn6966 from strain 81703, (vii) a Tn6397-related ICE Tn6967 from strain ZJG944, and (viii) a 35.8-kb Tn2670-related element T2670RE<sub>11759</sub> from strain 11759. All of these T10RE, T7RE, T1696RE, and T2670RE elements could not be recognized as intact transposons due to truncation of relevant core transposition modules. A detailed sequence comparison was applied to these 18 AGEs together with five prototype AGEs, Tn1696, Tn6963, Tn6872, Tn6397, and Tn2670 from GenBank (Table 2). At least 52 ARGs, involved in resistance to 15 different categories of antimicrobials, were identified in these 23 AGEs (Table S5).

**Two IS26/IS15DI-composite transposons, Tn6759 and Tn6760.** Tn6759 and Tn6760 (Fig. 5) from two *Morganella* isolates were inserted at different chromosomal locations and bracketed by 8-bp direct repeats (DRs; target site duplication signals for transposition). Tn6759 was bound by two copies of IS26, while Tn6760 was bound by two copies of IS15DI, and these two IS elements belonged to IS26 family and had only three point variation sites on their nucleotide sequences. Tn6759 and Tn6760 carried completely different antimicrobial resistance loci (ARLs): (i) a disrupted ISCR2–*flor* unit in Tn6759 and (ii) a type A In37-like element with a truncated gene cassette

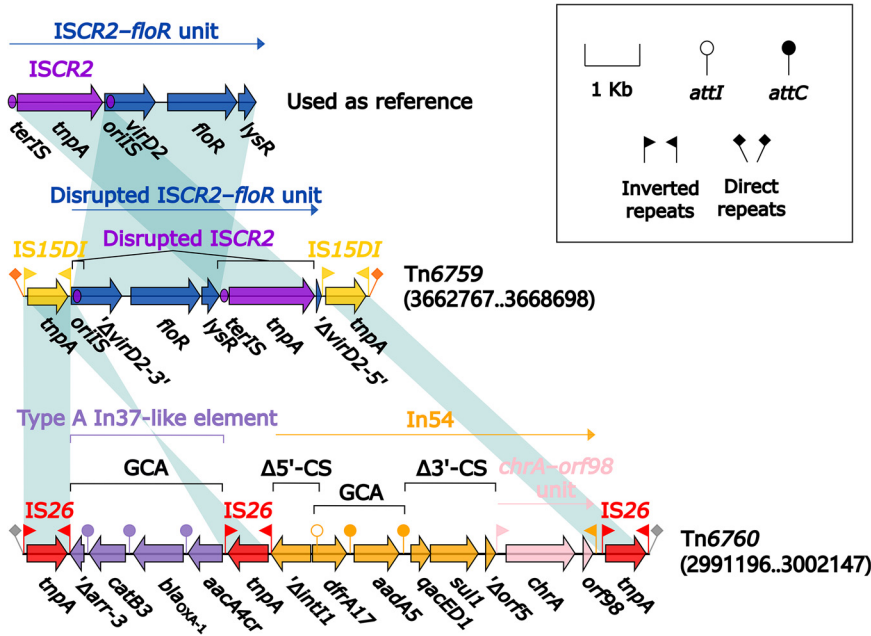


**FIG 5** Comparison of two IS26/IS15DI-composite transposons. Genes are denoted by arrows. Genes, AGEs, and other features are colored based on their functional classification. Shading denotes regions of homology (nucleotide identity  $\geq 95\%$ ). Numbers in brackets indicate nucleotide positions within the chromosomes of strains 11759 and 21164, respectively. Accession number of ISCR2-floR unit (53) used as reference is CP042857.

array (GCA) *aacA4cr*–*bla*<sub>OXA-1</sub>–*catB3*– $\Delta$ *arr-3*, plus a concise class 1 integron In54 with a GCA *dfrA17*–*aadA5* in Tn6760.

**Tn10 and its derivatives Tn6798, Tn6799, and T10RE<sub>GN28</sub>** Tn10 was initially described in *Shigella flexneri* plasmid R100, and it was a prototype IS10-composite transposon carrying a class B tetracycline-resistance module *tetRACD* (20). Here, Tn10 and its three derivatives (Fig. 6) from seven *Morganella* isolates were inserted at five different chromosomal locations and bracketed by 9-bp DRs. Compared to Tn10, its three derivatives underwent two major insertion events: (i) IS1R was inserted downstream of *ydhA* in Tn6798 and (ii) Tn2670-related transposon Tn6970 (see below) and 34.9-kb T2670RE<sub>GN28</sub> (see below) were inserted at the same site within *ydhA* in Tn6799 and T10RE<sub>GN28</sub>, respectively, leading to truncation of *ydhA* in Tn6799 and that of *ydhA* plus IS10L in T10RE<sub>GN28</sub>.

**Tn7 and its derivatives Tn6800 and T7RE<sub>621164</sub>** The prototype unit transposon Tn7 was initially found in *Escherichia coli* plasmid R483 and composed of the core transposition module *tnsABCDE* and a class 2 integron In2-4 (GCA: *dfrA1*–*sat2*–*aadA1*) (21). Here, Tn7 and its two derivatives (Fig. 7) from four *Morganella* isolates were integrated at the same chromosomal location and bracketed by 5-bp DRs. Tn6800 or T7RE<sub>621164</sub> differed from Tn7 by acquisition of In2-77 with GCA *Inu(F)1b*–*catB2*–*sat2*–*aadA1* or In2-16 with GCA *Inu(F)1b*–*catB2*–*sat2*–*aadA1*, respectively, instead of In2-4 (Fig. 5A). T7RE<sub>621164</sub> underwent an additional insertion event: a 31.1-kb multidrug resistance (MDR) region was inserted within *tnsD* (Tn7 target-site selection protein), leading to truncation of *tnsABCDE* (Fig. 7A). This MDR region (Fig. 7B) harbored two ARLs: IS26–*mph(E)*–IS26 unit and In1684. In1684 was a complex class 1 integron carrying *aacA4*–*bla*<sub>OXA-1</sub>–*catB3*–*arr-3* (GCA/VR1: variable region 1), a disrupted Tn2 containing *bla*<sub>TEM-1</sub>,  $\Delta$ Tn6502a containing *bla*<sub>CTX-M-3r</sub>, and VR2 (ISCR1–*qnrVC1* unit plus truncated ISCR1–*rmtB* unit).

**Five Tn1696 derivatives, Tn6913a, Tn6913b, Tn6914, Tn6915, and T1696RE<sub>ZJD581</sub>** Tn1696 was initially found in *Pseudomonas aeruginosa* plasmid R1033 (22). It was one of the Tn21-subfamily prototype unit transposons and had a backbone structure, IRL (inverted repeat left)–*tnpA* (transposase)–*tnpR* (resolvase)–*res* (resolution site)–*mer*

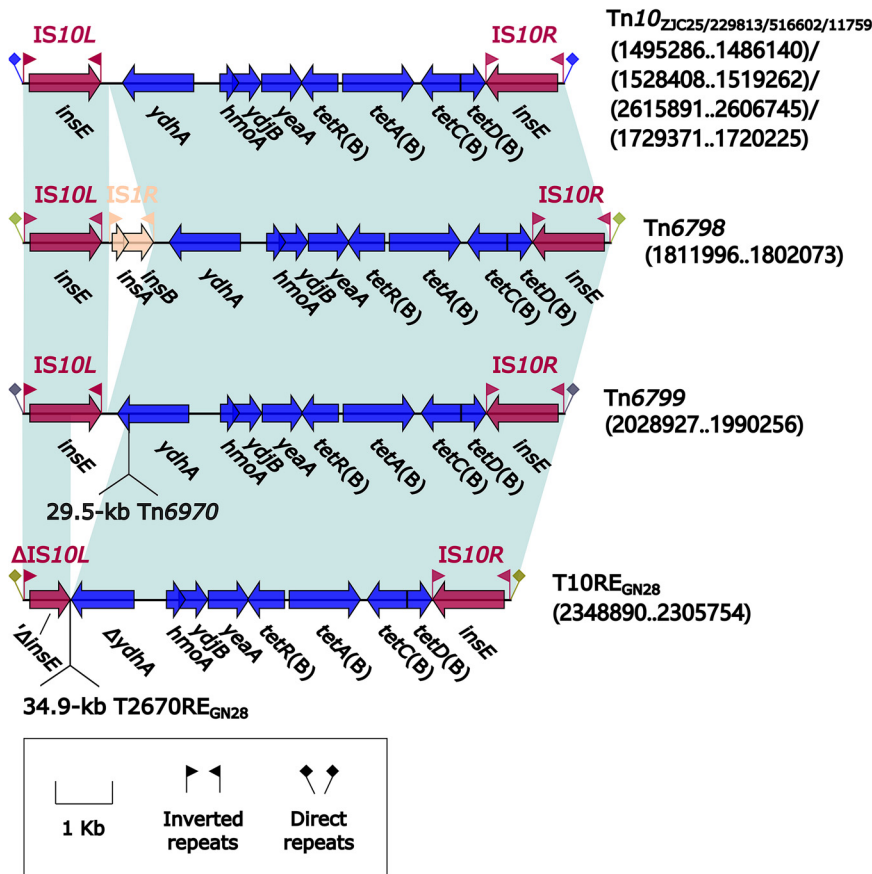


**FIG 6** Comparison of *Tn10* and its three derivatives. Genes are denoted by arrows. Genes, AGEs, and other features are colored based on their functional classification. Shading denotes regions of homology (nucleotide identity  $\geq 95\%$ ). Numbers in brackets indicate nucleotide positions within the chromosomes of strains ZJC25, 229813, 516602, 11759, 621164, 715304, and GN28, respectively.

(mercury resistance operon)–IRR (inverted repeat right), with integration of a class 1 integron In4 (GCA: *aacC1–gcuE–aadA2–cmlA1*) into *res* (23). Here, the five *Tn1696* derivatives (Fig. 8) from five *Morganella* isolates were inserted into three different chromosomal locations and bracketed by 5-bp DRs. Each of these five derivatives acquired a unique ARL instead of In4 in *Tn1696*: 38.9-kb T2670RE<sub>ZJG812</sub> (see below) in *Tn6913a*, 38.5-kb T2670RE<sub>ZJG944</sub> (see below) in *Tn6913b*, In1396 (GCA: *aadA13–gcuD*) in *Tn6914*, In1396 plus a 37.9-kb MDR region (see below) in *Tn6915*, and In1785 (VR1: *aadB–catB5f–bla<sub>OXA-10</sub>–aadA1dx*; VR2: *ISCR1–aphA6* unit) plus 39.6-kb MDR region (see below) in T1696RE<sub>ZJD581</sub>. Additionally, *tnpA* of T1696RE<sub>ZJD581</sub> was interrupted by *Tn6260:ISPmi3*.

**Two transposable prophages, Tn6963 and Tn6964.** The prototype transposable prophage *Tn6963* was initially found in *M. morganii* L241 (24). *Tn6963* and *Tn6964* (Fig. 9) shared conserved  $\lambda$  phage life cycle-related markers *attL/attR* (attachment sites at left/right ends), *int–xis* (integration and excision), *bet–to–cII* (lysogeny), *repO–dnaC* (DNA replication), *hol–lys* (lysis), *terSL–gpBC–cap–FI–FII* (head assembly), and *gpZVUGTHMLKIJ* (tail assembly) (25). *Tn6963* contained no accessory modules, while *Tn6964* acquired two: IS10-composite transposon *Tn6965* that harbored truncated *Tn10* carrying *tetRACD(B)* plus 39.4-kb MDR region (see below), and so called “inserted region” (26) that was cryptic and bracketed by 2-bp DRs.

**Two IMEs, Tn6872 and Tn6966.** The prototype IME *Tn6872* was initially found in *Providencia rustigianii* NCTC6933 (accession number [LR134189](#)). *Tn6872* and *Tn6966* (Fig. 10) shared core IME backbone markers *attL/attR*, *int*, and *oriT* (origin of conjugative replication), but they displayed dramatic modular variations cross the backbones: *Tn6872* had its unique regions *orf201* to *orf207*, *orf627* to *orf1068*, and *orf1338* to *uvrD*,

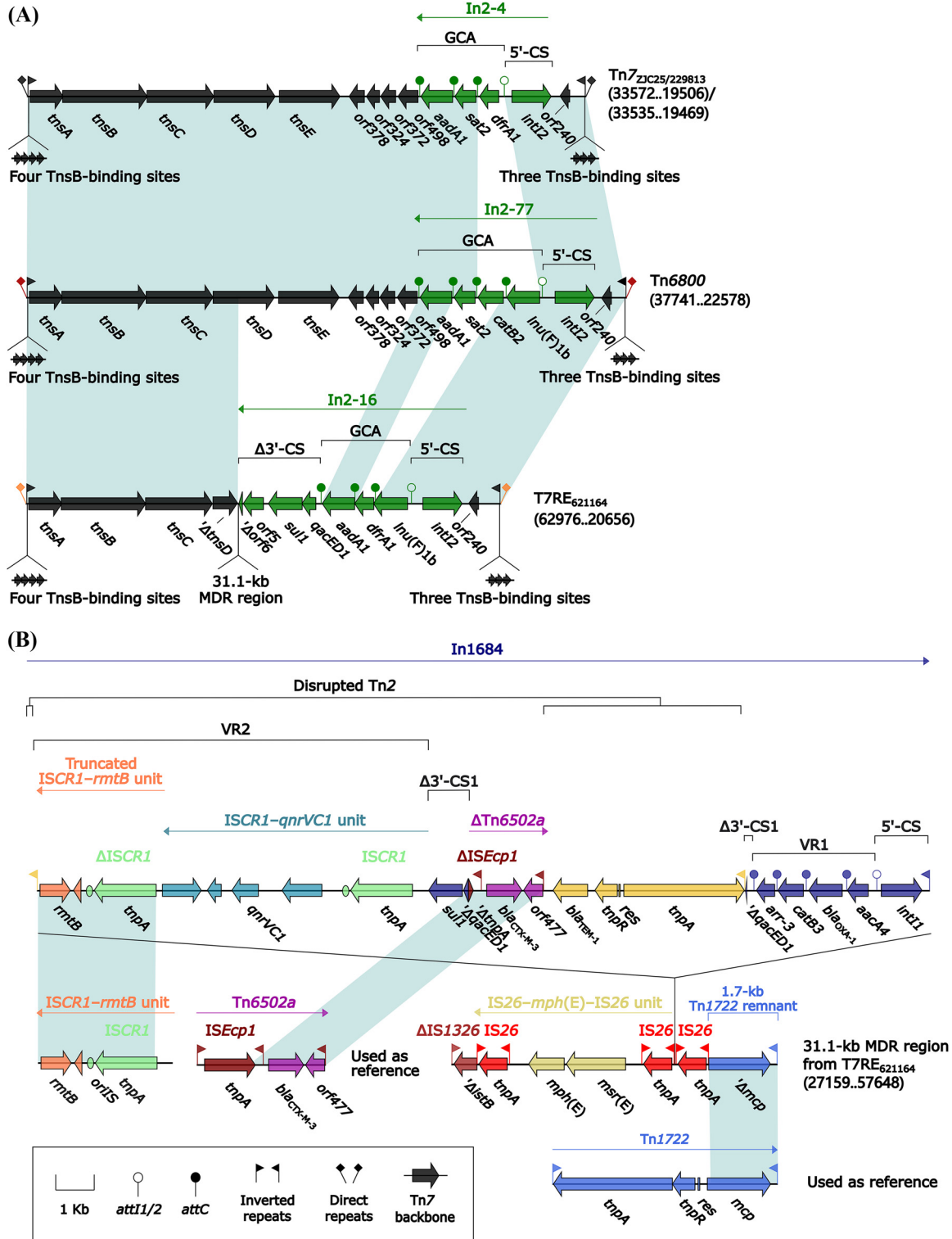


**FIG 7** Comparison of Tn7 and its two derivatives. (A) Organization of Tn7 and its two derivatives. (B) Organization of 31.1-kb MDR region from 42.3-kb T7RE<sub>621164</sub>. Genes are denoted by arrows. Genes, AGEs, and other features are colored based on their functional classification. Shading denotes regions of homology (nucleotide identity  $\geq 95\%$ ). Numbers in brackets indicate nucleotide positions within the chromosomes of strains ZJC25, 229813, 81703, and 621164, respectively. Accession numbers of ISCR1-rmtB unit, Tn6502a (54), and Tn1722 (55) are CP059348, KF914891, and X61367, respectively.

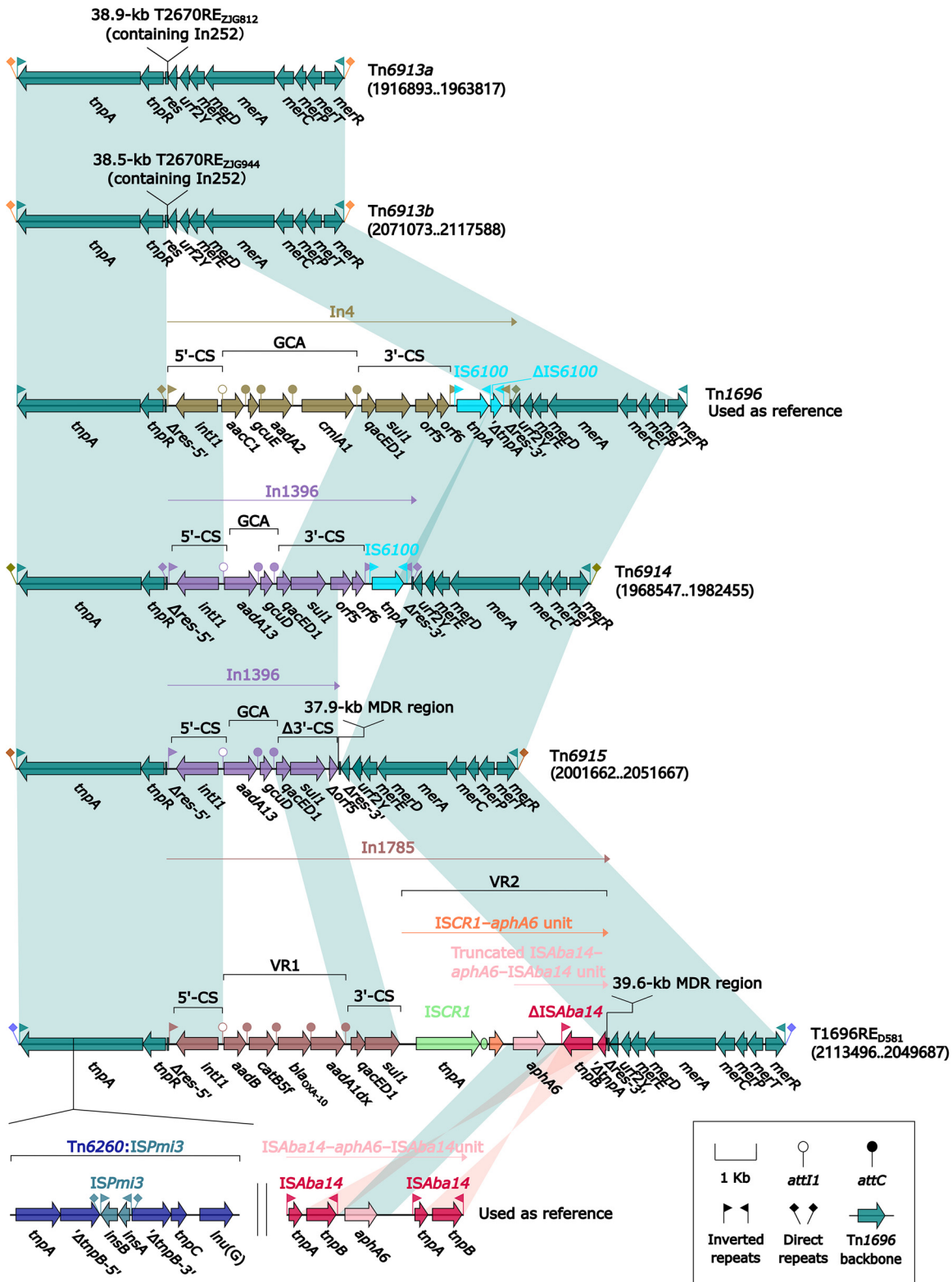


**FIG 8** Comparison of Tn1696 and its five derivatives. Genes are denoted by arrows. Genes, AGEs, and other features are colored based on their functional classification. Shading denotes regions of homology (nucleotide identity  $\geq 95\%$ ). Numbers in brackets indicate nucleotide positions within the chromosomes of strains ZJG944, ZJG812, ZJC25, Z29813, and ZJD581, respectively. Accession numbers of Tn1696 (22) and ISAbA14-aphA6-ISAbA14 unit (56) used as reference are U12338 and CP046406, respectively.

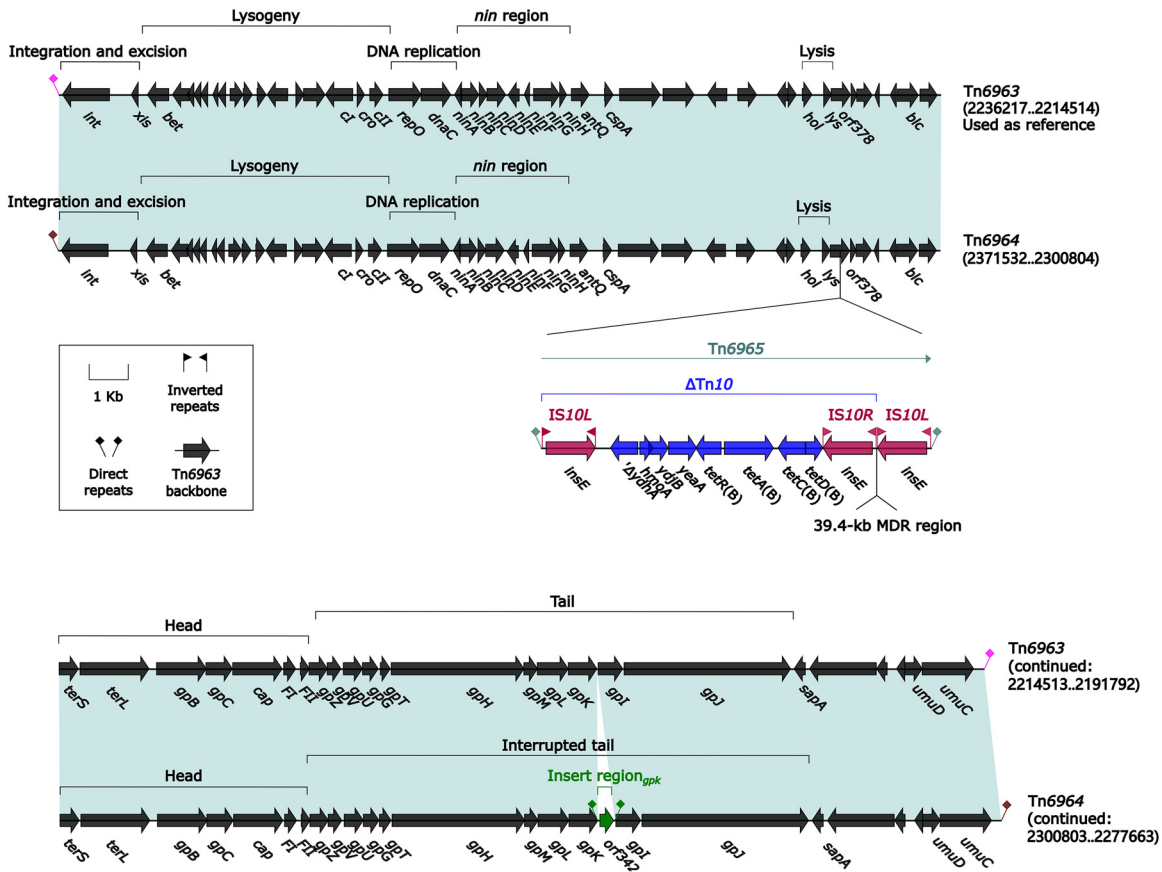


**FIG 9** Comparison of two Tn6963-related transposable prophages. Genes are denoted by arrows. Genes, AGEs, and other features are colored based on their functional classification. Shading denotes regions of homology (nucleotide identity  $\geq 95\%$ ). Numbers in brackets indicate nucleotide positions within the chromosomes of strains L241 and 12034, respectively. Accession number of Tn6963 (24) used as reference is CP033056.

while Tn6966 contained the counterparts *hsdMSR*–*mrr*–*orf411*, *orf597* to *orf1107*, and *orf1311* to *hnhc*, respectively. Tn6872 carried no accessory modules, while Tn6966 acquired two: *IS10R* and a region composed of 23.2-kb MDR region (see below) plus Tn21-related transposon Tn6971 (see below).

**Two ICEs, Tn6397 and Tn6967.** The prototype ICE Tn6397 was initially found in *Enterobacter* spp. A1137 (27). Tn6397 and Tn6967 (Fig. 11A) shared conserved ICE backbone markers *attL/attR*, *int*, *xis*, *rlx* (relaxase), *oriT*, *cpl* (coupling protein), and F (TivF)-type type IV secretion system gene set (mating pair formation). Tn6397 and Tn6967 each harbored a unique large accessory module (LAM) inserted at the same site within ICE backbones. These two LAMs (Fig. 11B) had similarity in gene organizations but exhibited totally different profiles of ARLs: (i) Tn1696-related transposon Tn6378 carrying *In73* (GCA: *bla*<sub>IMP-8</sub>–*aacA4*–3) plus macrolide-resistance locus *macAB*–*tolC* in 63.7-kb LAM of Tn6397 and (ii) a 20.9-kb MDR region (see below) plus a Tn21-related transposon Tn6972 (see below) in 48.5-kb LAM of Tn6967.

**Two Tn21-subfamily transposons, Tn6971 and Tn6972.** The sequence comparison (Fig. 12) was also applied to the two Tn21 derivatives Tn6971 and Tn6972 (identified as the inner components of Tn6966 and Tn6967, respectively; see above), together with Tn21 (28). Tn21, initially found in *Shigella flexneri* plasmid R100 (28), was another Tn21-subfamily prototype transposon, and it displayed the backbone structure IRL–*tnpAR*–*res*–*mer*–IRR with the integration of *In2*. Tn6971 and Tn6972 (Fig. 12) harbored Tn21 core transposition determinants *tnpAR* and IRL/IRR, but Tn1696 *mer* locus, instead of that in Tn21, was found in Tn6971, while Tn6972 did not contain *mer*. Tn6971 and Tn6972 each acquired a unique ARL: *In1086* [which had GCA *aacA4cr*–*bla*<sub>OXA-1</sub>–*catB3*–

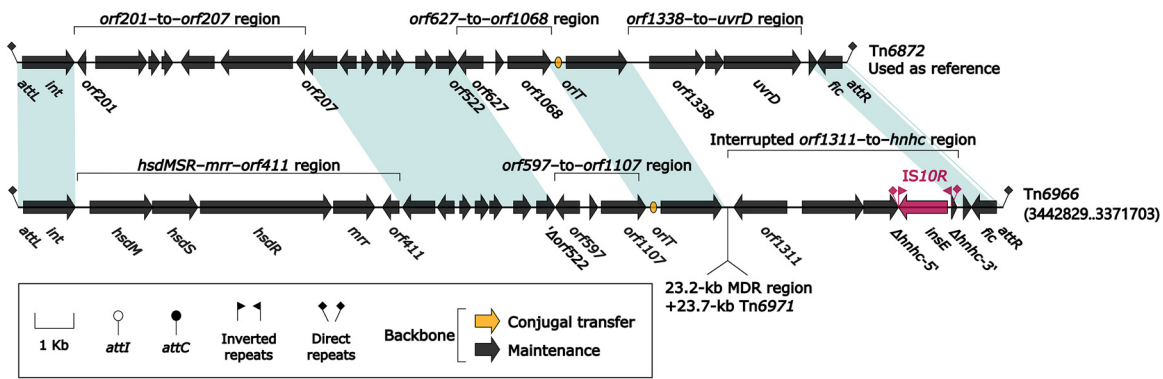


**FIG 10** Comparison of two Tn6872-related IMEs. Genes are denoted by arrows. Genes, AGEs, and other features are colored based on their functional classification. Shading denotes regions of homology (nucleotide identity  $\geq 94\%$ ). Numbers in brackets indicate nucleotide positions within the chromosome of strain 81703. Accession number of Tn6872 used as reference is [LR134189](https://pub.ncbi.nlm.nih.gov/record/CP013418).

*arr-3-dfrA27-aadA16* and was additionally inserted with *tetRACD(B)*-carrying  $\Delta$ Tn10 in Tn6971 and *macAB-toIC* in Tn6972].

**Five Tn2670 derivatives, Tn6970, T2670RE<sub>11759</sub>, T2670RE<sub>GN28</sub>, T2670RE<sub>ZJG812</sub>, and T2670RE<sub>ZJG944</sub>.** The sequence comparison (Fig. 13) was also applied to five Tn2670 derivatives, Tn6970, T2670RE<sub>11759</sub>, T2670RE<sub>GN28</sub>, T2670RE<sub>ZJG812</sub>, and T2670RE<sub>ZJG944</sub>, together with Tn2670 (28). T2670RE<sub>11759</sub> was directly integrated into the chromosome, while the remaining four were recognized as the inner components of Tn10 derivatives Tn6799 and T10RE<sub>GN28</sub> and Tn1696 derivatives Tn6913a and Tn6913b (see above). Tn2670 was an IS1R-composite transposon composed of a Tn9-like backbone (29) with the integration of Tn21 (30), and it was initially found in *Shigella flexneri* plasmid R100 (28). Compared to Tn2670, Tn6970, T2670RE<sub>ZJG812</sub>, and T2670RE<sub>ZJG944</sub> harbored the same intact Tn9-like backbone but contained different versions of truncated Tn21 with integration of two different integrons: (i) In299 [GCA: *Inu(F)1b-catB2-sat2-aadA1*] inserted with In313 (VR1: *bla<sub>CARB-2</sub>-aadA2* and VR2: *ISCR1-ΔISCR1-ligA-dfrA19*) in Tn6970 and (ii) In252 (VR1: *aadB-catB5-bla<sub>OXA-10</sub>-aadA1a*; VR2: *ISCR1-qnrVC1* unit) in T2670RE<sub>ZJG812</sub> and T2670RE<sub>ZJG944</sub>. T2670RE<sub>11759</sub> and T2670RE<sub>GN28</sub> contained the whole 5'-terminal Tn9-like backbone and a very small Tn21 remnant; moreover, each of them acquired a unique LAM, the resulting two LAMs shared one ARL [*IS26-mpH(A)-IS6100* unit], and each LAM further acquired five or four different ARLs: (i) In54, 1.4-kb truncated *aacC2-tmrB* region, Tn6029 (containing *bla<sub>TEM-1</sub>, sul2, strA, and strB*) interrupted by Tn4352 (containing *aphA1*), truncated type A *IS26-fosA3-IS26* unit, and type A In37-like element in T2670RE<sub>11759</sub> and (ii) type B In37-like element (GCA: *aacA4cr-bla<sub>OXA-1</sub>-catB3-arr-3*), 3.3-kb truncated *aacC2-tmrB* region, In313 (GCA: *bla<sub>CARB-2</sub>-aadA2*), and *ISCR3-ereB* unit in T2670RE<sub>GN28</sub>. Notably, eight and five copies of *IS26/IS15DI* and *IS6100* were presented in T2670RE<sub>11759</sub> and T2670RE<sub>GN28</sub>, respectively; all these IS elements belonged to IS6 family and possessed almost identical 14-bp IR sequences, and thus they would be together involved in complex homologous recombination events, promoting the assembly of LAMs in T2670RE<sub>11759</sub> and T2670RE<sub>GN28</sub>.

**Five *aacC4/aph(4)-la/sul2/floR*-carrying MDR regions.** The sequence comparison (Fig. 14) was also applied to five different MDR regions (identified as the inner components of Tn6967, Tn6915, T1696RE<sub>ZJD581</sub>, Tn6966, and Tn6965, respectively; see above), which shared 15.5/16.0-kb *aacC4/aph(4)-la/sul2/floR*-carrying region. All these 15.5/16.0-kb regions comprised three major ARLs: *IS26-aacC4-aph(4)-la-ISEc59*, *ISCR2-sul2* unit, and truncated *ISCR2-floR* unit. In addition, each of these five MDR regions integrated one or more additional ARLs: (i) In37, type C In37-like element, and type D (all contained the intact GCA *aacA4cr-bla<sub>OXA-1</sub>-catB3-arr-3*) in MDR regions from T1696RE<sub>ZJD581</sub>, Tn6967, and Tn6915, respectively, (ii) In27 (GCA: *dfrA12-aadA2*) plus *aphA1*-containing  $\Delta$ Tn4352 as shared by MDR regions from T1696RE<sub>ZJD581</sub>, Tn6966, and Tn6965, (iii) truncated *IS26-mef(B)-sul3-IS440* unit and In641 (GCA: *aadA2-cmlA1a-*

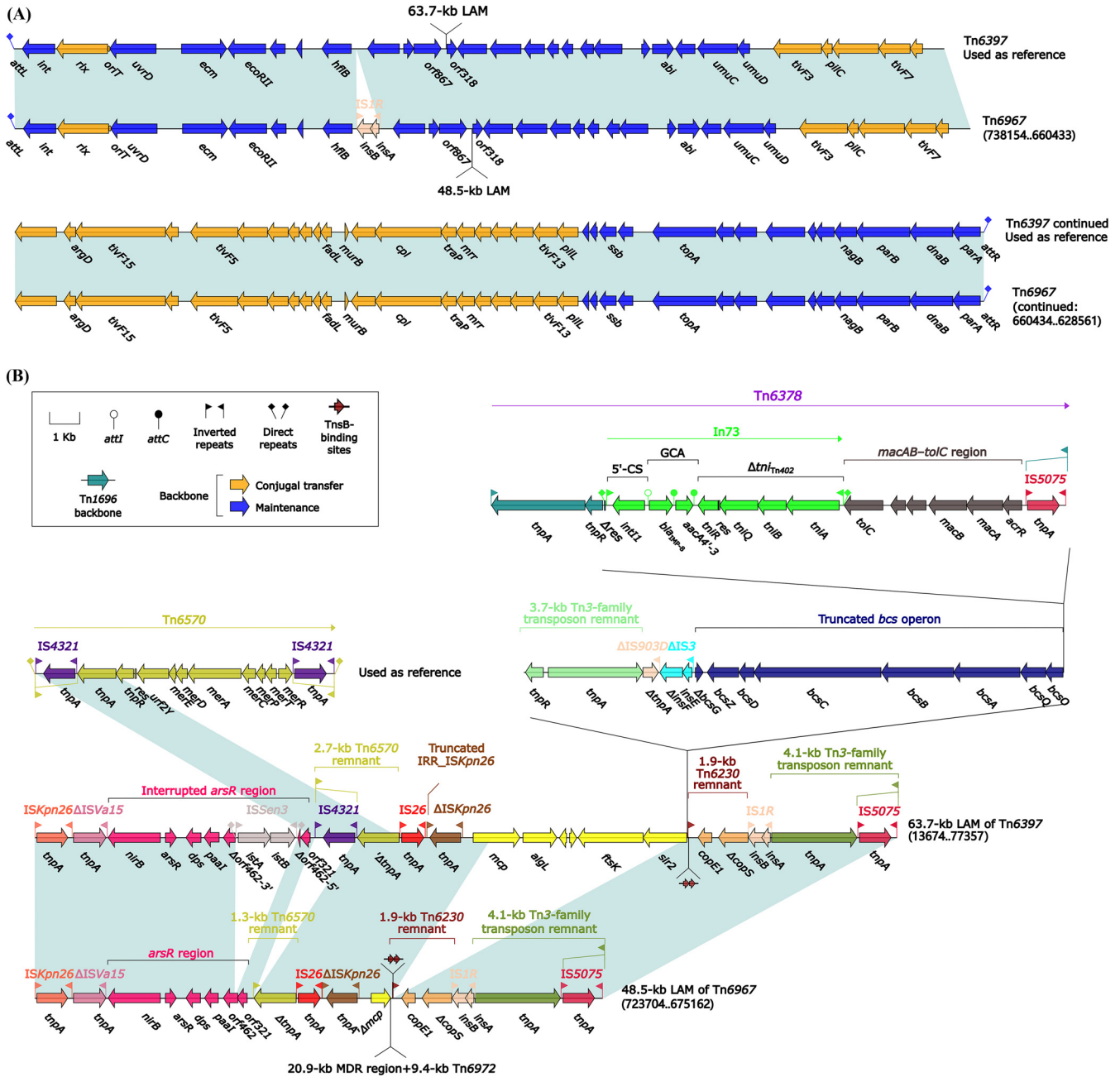


**FIG 11** Comparison of two Tn6397-related ICEs. (A) Organization of Tn6397 and Tn6967. (B) Organization of LAMs of Tn6397 and Tn6967. Genes are denoted by arrows. Genes, mobile elements, and other features are colored based on their functional classification. Shading denotes regions of homology (nucleotide identity ≥ 95%). Numbers in brackets indicate nucleotide positions within the chromosome of strain ZJG944. Accession numbers of Tn6397 (27) and Tn6570 used as reference are CP021851 and CP043397, respectively.

*aadA1a-qach2*) in MDR region from Tn6915, and (iv) *In1787* (GCA: *aacA4cr12-bla*<sub>OXA-1</sub>-*catB3-arr-3-dfrA27-aadA16*) in MDR region from Tn6965.

**Newly identified or designated AGEs.** There were 19 newly identified AGEs in total: (i) 12 of them directly integrated into the chromosomes and included 4 composite transposons, Tn6759, Tn6760, Tn6798, and Tn6799, 5 unit transposons, Tn6800, Tn6913a, Tn6913b, Tn6914, and Tn6915, 1 transposable prophage, Tn6964, 1 IME, Tn6966, and 1 ICE, Tn6967, and (ii) the remaining 7 were the inner components of the above 12 and comprised 2 composite transposons, Tn6965 and Tn6970, 2 unit transposons, Tn6971 and Tn6972, and 3 integrons, *In2-77*, *In1785*, and *In1787*. Additionally, there were two newly designated (first designated in this study but with previously determined sequences)

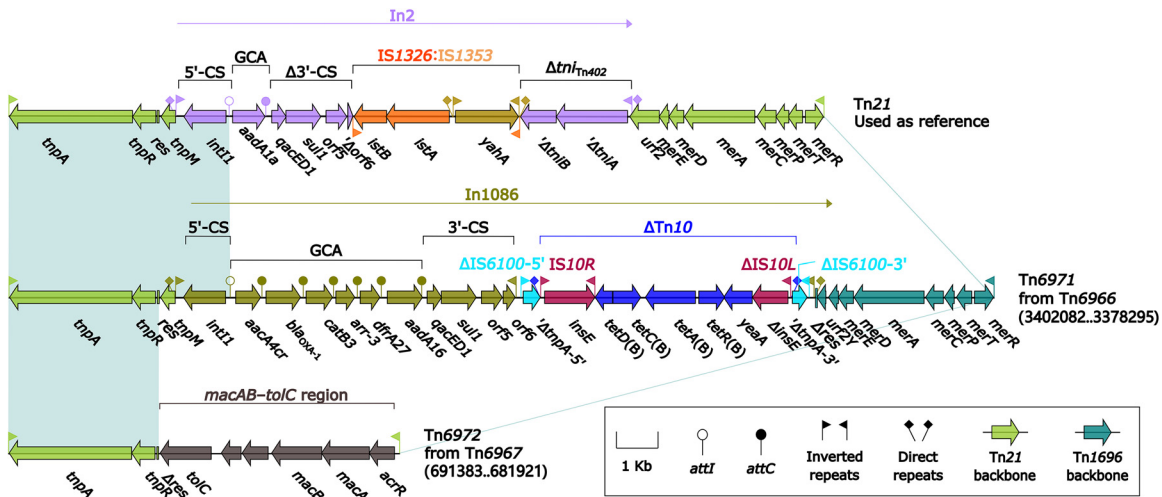


**FIG 12** Comparison of Tn21 and its two derivatives. Genes are denoted by arrows. Genes, AGEs, and other features are colored based on their functional classification. Shading denotes regions of homology (nucleotide identity  $\geq 95\%$ ). Numbers in brackets indicate nucleotide positions within the chromosomes of strains 81703 and ZJG944, respectively. Accession number of Tn21 (28) is AF071413.

AGEs: 1 putative resistance unit, ISCR3-ere(B) unit, and 1 transposable prophage, Tn6963. All these 21 newly identified or designated AGEs were first identified in the 166 global *Morganella* isolates. Additionally, Tn6872-related IME, Tn6397-related ICE, and ARG-harboring Tn6963-related transposable prophage were reported for the first time in *Morganella*.

**DISCUSSION**

There are few reports on characterizing ARGs in individual *Morganella* isolates or a small collection of *Morganella* isolates ( $n \leq 22$  in each study) (31–33). This study provides a genomic and bioinformatics view of the classification and evolution of *Morganella* species and the global prevalence of AGEs and associated ARGs in *Morganella*, based on a collection of 166 sequenced isolates, including 60 sequenced in this study.

We establish a systematic genome sequence-based species classification scheme for *Morganella* based on ANI analysis plus phylogenomic analysis. The two conventional *Morganella* species, *M. morganii* and *M. psychrotolerans*, should be redefined as two complexes: *M. morganii* and *M. psychrotolerans*, which can be further divided into four and two genospecies, respectively. These two complexes display a very long-distance phylogenomic relationship, being consistent with a previous phylogenetic analysis based on seven *Morganella* housekeeping genes (2). Moreover, the six genospecies display the obvious segregation at genome scale between each other, as revealed by ANI analysis and further confirmed by phylogenomic assay. Notably, all these genospecies cannot be distinguished based on the sequence variation of 16S rRNA genes or that of the seven housekeeping genes (2, 34). Isolates of *M. morganii* genospecies can be mostly frequently recovered from patients, animals, and the environment, accounting for 147 (91.9%) of the total 160 strains studied. Our phylogenomic analysis on these 147 global isolates of *M. morganii* genospecies shows that this genospecies exhibits a highly clonal population disseminated across at least 16 countries of the five continents (Table S1). These 147 isolates gather at the farthest position from the root in the phylogenetic tree, and therefore *M. morganii* genospecies represents the latest differentiated clone among all the six genospecies.

Of these 88 acquired ARGs, the most prevalent are tetracycline-resistance tetAR genes, which are found in 99 (59.64%) of the 166 isolates studied. Tetracycline antibiotics have been extensively used in treatment of human and animal infections for at least 60 years (35). The long-term use of tetracycline antibiotics promotes the acquisition

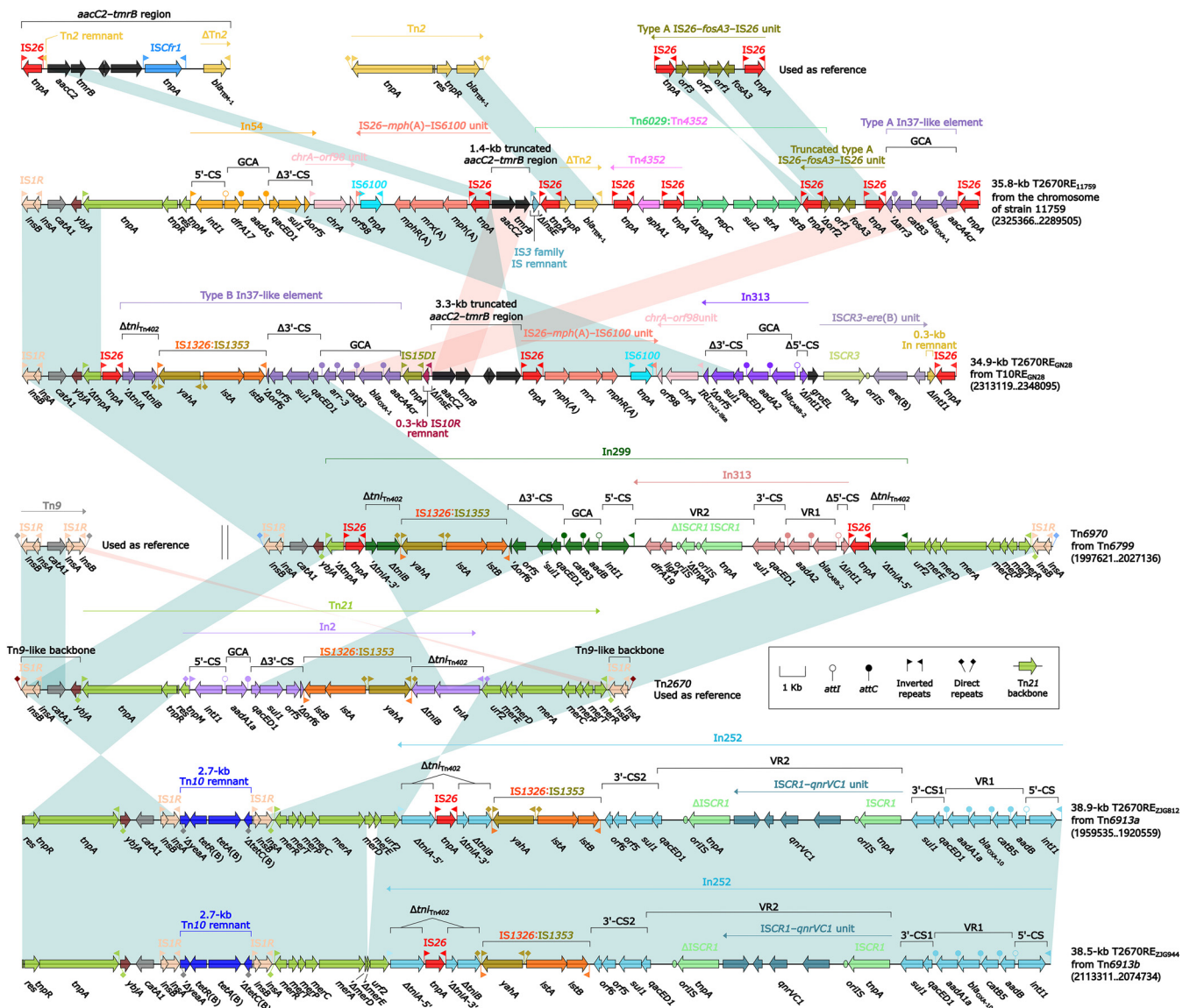


**FIG 13** Comparison of Tn2670 and its five derivatives. Genes are denoted by arrows. Genes, AGEs, and other features are colored based on their functional classification. Shading denotes regions of homology (nucleotide identity  $\geq 95\%$ ). Numbers in brackets indicate nucleotide positions within the chromosomes of strains 11759, GN28, 81703, ZJG944, and ZJG812, respectively. Accession numbers of *aacC2*-*tmrB* region (57), Tn2 (58), type A IS26-*fosA3*-IS26 unit (59), Tn9 (29), Tn2670 (28), and Tn10 (20) used as reference are [JX101693](#), [X64367](#), [KP987215](#), [V00622](#), [AP000342](#), and [AP000342](#), respectively.

and dissemination of tetracycline-resistance genes in various bacteria, such as *Acinetobacter*, *Escherichia*, and *Salmonella* (36), and also *Morganella*, here. In addition, the wide prevalence of  $\beta$ -lactam-resistance genes is also observed in *Morganella* isolates ( $n = 58$ , 34.93%), which might be due to the frequent empirical use of cephalosporins for clinical therapy of *M. morganii*-induced infections (37).

The 60 isolates sequenced in this study exhibit the highest nonsusceptibility rate ( $n = 40$ , 66.67%) for levofloxacin and ciprofloxacin. There are three major mechanisms of fluoroquinolone resistance in *Morganella*: (i) acquisition of quinolone-resistance genes *qnr* (12), *qepA* (38), and *aacA4cr* (39), (ii) mutation of type II topoisomerases genes *gyrAB* and *parCE* (40, 41), and (iii) enhancement of proton-dependent active effluxes (42). A total of 31 of these 60 isolates carry acquired *qnr* and/or *aacA4cr* genes, but only 17 of these 31 isolates are nonsusceptible to fluoroquinolones (Table S1). Commonly, the carriage of *qnr*, *qepA*, and *aacA4cr* genes only mediates limited decreased susceptibility to fluoroquinolones but cannot guarantee that the isolates exhibit the fluoroquinolone resistance with a breakpoint of 0.5  $\mu\text{g}/\text{mL}$  provided by Clinical and Laboratory Standards

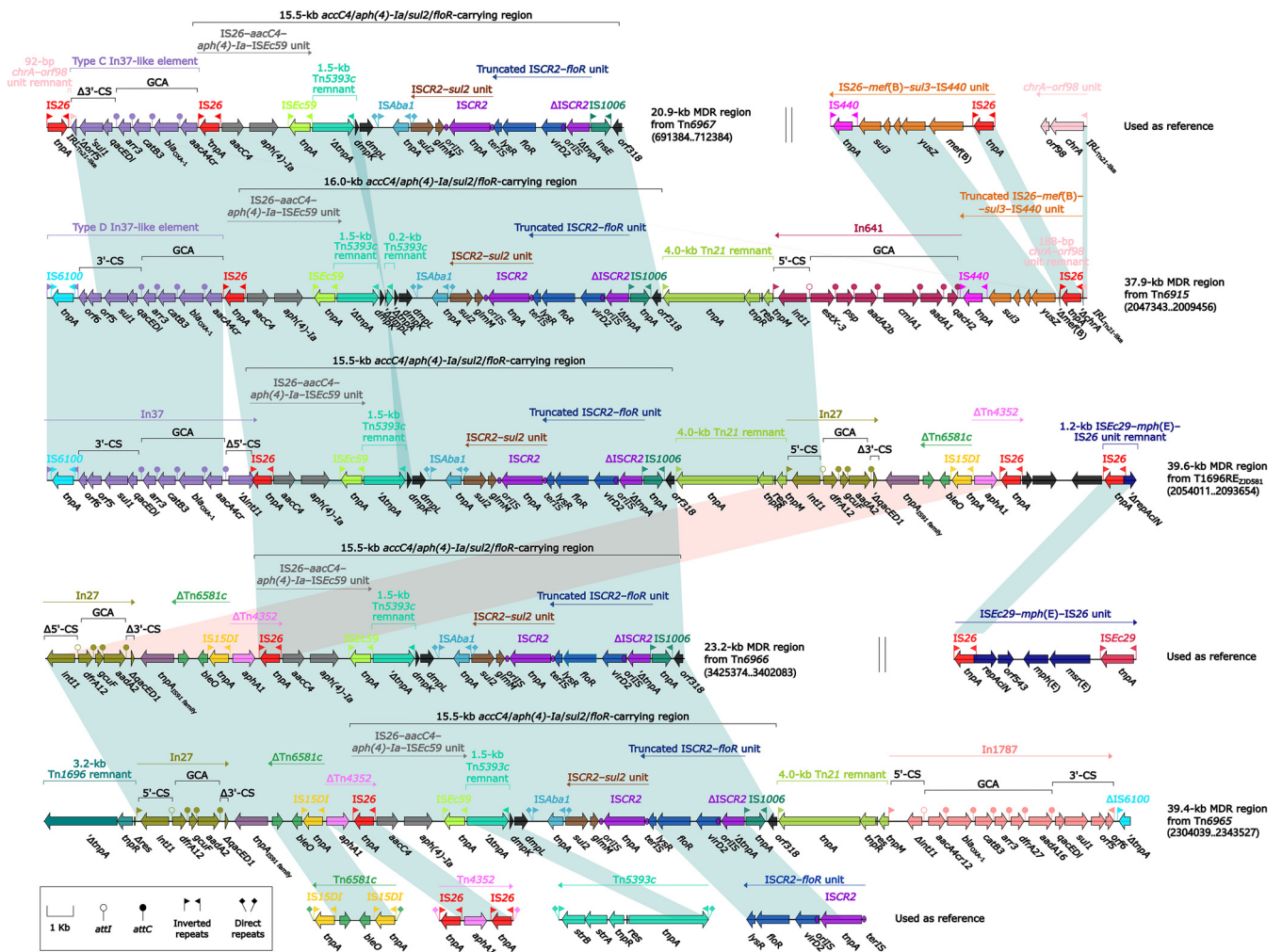


**FIG 14** Comparison of five *aacC4/aph(4)-Ia/sul2/floR*-carrying MDR regions. Genes are denoted by arrows. Genes, AGEs, and other features are colored based on their functional classification. Shading denotes regions of homology (nucleotide identity  $\geq 95\%$ ). Numbers in brackets indicate nucleotide positions within the chromosomes of strains ZJG944, 229813, ZJD581, 81703, and 12034, respectively. Accession numbers of IS26–*mef(B)*–*sul3*–IS440 unit (60), *chrA*–*orf98* unit (53), IS29–*mph(E)*–IS26 unit (61), Tn6581c, Tn4352 (62), Tn5393c (63), and ISCR2–*floR* unit (53) are FJ196385, CP042858, AF550415, CP042857, CP042858, AF262622, and CP042857, respectively.

Institute (CLSI) (43, 44). It is speculated that the extensive nonsusceptibility for fluoroquinolones in *Morganella* isolates is most likely caused by the combination of the above multiple resistance mechanisms.

The lowest nonsusceptibility rates were observed for meropenem ( $n = 6$ , 10%) and amikacin ( $n = 3$ , 5%) in these 60 Chinese isolates. Similar results were found for the 692 *Morganella* isolates from China Antimicrobial Surveillance Network (Table S7). These denote that carbapenems and amikacin will be the most effective antimicrobials against *Morganella* in China. The observed meropenem resistance and amikacin resistance in the above six and three *Morganella* isolates are mediated by the acquisition of carbapenemase gene (*bla*<sub>KPC-2</sub> [ $n = 4$ ] or *bla*<sub>NDM-1</sub> [ $n = 2$ ]) and 16S rRNA methyltransferase gene (*rmtB*), respectively. The presence of carbapenemase genes or *rmt* gene can be identified in only 21 of these 166 global *Morganella* isolates (Table S1). Taken together, meropenem resistance or amikacin resistance is still not widely disseminated in *Morganella*.

This study presents the full sequences of 18 AGEs located within *Morganella* chromosomes. Subsequently, a detailed sequence comparison was applied to these 18 AGEs, together with 5 additional prototype AGEs from GenBank. These 23 AGEs could be divided into eight distinct groups: two IS26/IS15DI-composite transposons, Tn10 and its three

derivatives, Tn7 and its two derivatives, Tn1696 and its five derivatives, Tn6963 and its one derivative, Tn6872 and its one derivative, Tn6397 and its one derivative, and Tn2670 and its one derivative. Eleven of these 23 AGEs each carries a distinct LAM (>29.5 kb) with complex mosaic structure: (i) LAMs of Tn6799, T10RE<sub>GN28</sub>, Tn6913a, and Tn6913b manifest as distinct Tn2670-related elements, (ii) those of T7RE<sub>621164r</sub>, Tn6915, and T1696RE<sub>ZJD581</sub> contained different MDR regions, (iii) that of Tn6964 manifests as Tn6965 integrated with MDR region, (iv) that of Tn6966 comprises Tn6971 and MDR region, (v) that of Tn6967 contains Tn6972 and MDR region, and (vi) T2670RE<sub>11759</sub> as a LAM directly integrates into the chromosome. These LAMs are likely assembled from complex transposition and homologous recombination and, notably, comprise various ARLs, including composite/unit transposons, integrons, and putative resistance units, resulting in accumulation of at least 44 ARGs in *Morganella* chromosomes.

In summary, a genomic epidemiology analysis on 166 global sequenced *Morganella* isolates, including 60 sequenced here, was conducted in this study. First, a genome sequence-based species classification scheme for *Morganella* was established, and the two conventional *Morganella* species were redefined as two complexes, which were further divided into four and two genospecies, respectively. Second, the prevalence of acquired ARGs was screened based on genome sequences, demonstrating that at least 88 acquired ARGs are accumulated and disseminated in *Morganella*. Finally, a detailed sequence comparison of eight groups of 23 AGEs (including 18 *Morganella* chromosomal AGEs sequenced in this study) was performed. There are LAMs in 11 of these 23 AGEs, and these LAMs have complex mosaic structures and contain many ARLs and associated ARGs. Integration of these ARG-containing AGEs into *Morganella* chromosomes would contribute to the accumulation and dissemination of ARGs in *Morganella* and enhance the adaptation and survival of *Morganella* under complex and diverse antimicrobial selection pressures.

## MATERIALS AND METHODS

**Bacterial isolates and identification.** A total of 60 *Morganella* isolates were collected from 2013 to 2019, including 56 from hospitalized patients in seven Chinese public hospitals and 4 from animals in four Chinese farms (Table S1). The 16S rRNA genes and the carbapenemase genes *bla*<sub>NDM-1</sub> and *bla*<sub>KPC-2</sub> were detected as described previously (45). The activity of class A/B/D carbapenemases in bacterial cell extracts was detected by a modified CarbaNP test (45). The bacterial antimicrobial susceptibility was tested using bioMérieux Vitek 2 and interpreted as per the 2020 CLSI guidelines (44).

**Genomic DNA sequencing and sequence assembly and annotation.** All these 60 isolates were subjected to draft-genome sequencing using a paired-end library with an average insert size of 350 bp (ranged from 150 bp to 600 bp) on a HiSeq sequencer (Illumina, CA, USA). In addition, 12 (Table S1) of them were subjected to complete-genome sequencing with a sheared DNA library with an average size of 15 kb (ranged from 10 kb to 20 kb) on a PacBio RSII sequencer (Pacific Biosciences, CA, USA). The quality control analysis of sequencing data was conducted using NanoPack (46) and FastQC (<https://www.bioinformatics.babraham.ac.uk/projects/fastqc>). Sequence assembly and annotation were performed as described previously (47).

**ANI analysis and phylogenomic analysis.** The pairwise ANI values of *Morganella* genome sequences were calculated using FastANI (48). *Morganella* genome sequences were aligned to the complete chromosome sequence (accession number CP004345) of *M. morganii* subsp. *morganii* isolate KT used as reference, and the SNPs were identified by Mummer v3.25 (49). All the SNPs in the repetitive DNA regions were identified and filtered by RepeatMasker (<http://www.repeatmasker.org/>). Homologous recombination at a genome-wide level was predicted using ClonalFrameML (50), followed by removal of all putative recombinant SNP sites. Based on the final recombination-free core SNPs, a maximum-likelihood phylogenetic tree was constructed using RAxML (51) with a bootstrap iteration of 1,000 and displayed using iTOL (<https://itol.embl.de>).

**In silico analysis of prevalence of AGEs.** We collected the core transposition determinants (encoding transposases and their auxiliary factors) of the 17 major AGE groups, which were frequently found in Gram-negative bacteria (19). These 17 groups included IS26/IS15DI, IS10, and IS1R (highly associated with composite transposons) and Tn3-family (including Tn3, Tn21, Tn163, Tn4430, Tn4651, and Tn4401 subfamilies), Tn7-family (composed of Tn7, Tn6230, Tn552, Tn6022, and Tn5035 subfamilies), and Tn554-family (comprising Tn554, Tn6488, and Tn6571 subfamilies) unit transposons, as shown in our unpublished DANMEL database ([https://39.100.87.11/danmel\\_V1.0/index.php](https://39.100.87.11/danmel_V1.0/index.php)). The sequence alignment of these core transposition determinants was conducted on the draft-genome sequences of these 166 *Morganella* isolates, screening for the prevalence of these 17 major group AGEs in *Morganella*.

**Statistical analysis.** The statistical differences for ARGs among reservoirs were tested by Pearson's  $\chi^2$  test. Statistical computations and figures were plotted with R package v.3.271 (<http://www.r-project.org>) and visualized with Adobe Illustrator.

**Data availability.** The complete chromosome sequences of the 12 fully sequenced isolates 11759, 516602, ZJC25, 229813, 621164, 715394, GN28, 81703, ZJG944, ZJG812, ZJD581, and 12304 were submitted to GenBank under accession numbers CP059986, CP064054, CP064828, CP043955, CP064829, CP064833, CP064055, CP064830, CP064827, CP064831, CP064826, and CP064832, respectively. The GenBank accession numbers of all the plasmids of these 12 isolates are listed in Table S1. The draft-genome sequences were submitted to GenBank under BioProject PRJNA671578.

## SUPPLEMENTAL MATERIAL

Supplemental material is available online only.

**SUPPLEMENTAL FILE 1**, PDF file, 5.8 MB.

## ACKNOWLEDGMENTS

This work was supported by the National Natural Science Foundation of China (grant no. 3214100027).

## REFERENCES

- Adeolu M, Alnajjar S, Naushad S, S Gupta R. 2016. Genome-based phylogeny and taxonomy of the 'Enterobacteriales': proposal for Enterobacterales ord. nov. divided into the families Enterobacteriaceae, Erwiniaceae fam. nov., Pectobacteriaceae fam. nov., Yersiniaceae fam. nov., Hafniaceae fam. nov., Morganellaceae fam. nov. *Int J Syst Evol Microbiol* 66:5575–5599. <https://doi.org/10.1099/ijsem.0.001485>.
- Emborg J, Dalgaard P, Ahrens P. 2006. *Morganella psychrotolerans* sp. nov., a histamine-producing bacterium isolated from various seafoods. *Int J Syst Evol Microbiol* 56:2473–2479. <https://doi.org/10.1099/ijms.0.64357-0>.
- Jensen KT, Frederiksen W, Hickman-Brenner FW, Steigerwalt AG, Brenner DJ. 1992. Recognition of *Morganella* subspecies, with proposal of *Morganella morgani* subsp. nov. and *Morganella morgani* subsp. *sibonii* subsp. nov. *Int J Syst Evol Microbiol* 42:613–620.
- Edgar RC. 2018. Updating the 97% identity threshold for 16S ribosomal RNA OTUs. *Bioinformatics* 34:2371–2375. <https://doi.org/10.1093/bioinformatics/bty113>.
- Oh WT, Jun JW, Giri SS, Yun S, Kim HJ, Kim SG, Kim SW, Kang JW, Han SJ, Kwon J, Park SC. 2020. *Morganella psychrotolerans* as a possible opportunistic pathogen in rainbow trout (*Oncorhynchus mykiss*) fisheries. *Aquaculture* 520:735021. <https://doi.org/10.1016/j.aquaculture.2020.735021>.
- Liu H, Zhu J, Hu Q, Rao X. 2016. *Morganella morgani*, a non-negligent opportunistic pathogen. *Int J Infect Dis* 50:10–17. <https://doi.org/10.1016/j.ijid.2016.07.006>.
- Chen Y, Lei C, Zuo L, Kong L, Kang Z, Zeng J, Zhang X, Wang H. 2019. A novel cfr-carrying Tn7 transposon derivative characterized in *Morganella morgani* of swine origin in China. *J Antimicrob Chemother* 74:603–606. <https://doi.org/10.1093/jac/dky494>.
- Bing L, Jiao F, Zhe Z, Zhe Y, Zhou D. 2018. Dissemination of KPC-2-encoding IncX6 plasmids among multiple Enterobacteriaceae species in a single Chinese hospital. *Front Microbiol* 9:478. <https://doi.org/10.3389/fmicb.2018.00478>.
- Flannery EL, Mody L, Mobley HLT. 2009. Identification of a modular pathogenicity island that is widespread among urease-producing uropathogens and shares features with a diverse group of mobile elements. *Infect Immun* 77:4887–4894. <https://doi.org/10.1128/IAI.00705-09>.
- Xiang R, Li M. 2021. Identification of Tn6835 and a novel genomic island, MMGI-1, in a pan-resistant *Morganella morgani* strain. *Antimicrob Agents Chemother* 65:e02524-20. <https://doi.org/10.1128/AAC.02524-20>.
- Schultz E, Barraud O, Madec J-Y, Haenni M, Cloeckaert A, Ploy M-C, Doublet B. 2017. Multidrug resistance genomic island 1 in a subsp. human clinical isolate from France. *mSphere* 2. <https://doi.org/10.1128/mSphere.00118-17>.
- Mazzariol A, Kocsis B, Koncan R, Kocsis E, Lanzafame P, Cornaglia G. 2012. Description and plasmid characterization of *qnrD* determinants in *Proteus mirabilis* and *Morganella morgani*. *Clin Microbiol Infect* 18:E46–E48. <https://doi.org/10.1111/j.1469-0691.2011.03728.x>.
- Schöck F, Dahl MK. 1996. Expression of the *tre* operon of *Bacillus subtilis* 168 is regulated by the repressor TreR. *J Bacteriol* 178:4576–4581. <https://doi.org/10.1128/jb.178.15.4576-4581.1996>.
- Richter M, Rossello-Mora R. 2009. Shifting the genomic gold standard for the prokaryotic species definition. *Proc Natl Acad Sci U S A* 106:19126–19131. <https://doi.org/10.1073/pnas.0906412106>.
- Vos M, Didelot X. 2009. A comparison of homologous recombination rates in bacteria and archaea. *ISME J* 3:199–208. <https://doi.org/10.1038/ismej.2008.93>.
- Soltis PS, Soltis DE. 2003. Applying the bootstrap in phylogeny reconstruction. *Statist Sci* 18:256–267. <https://doi.org/10.1214/ss/1063994980>.
- Ramirez MS, Tolmasky ME. 2017. Amikacin: uses, resistance, and prospects for inhibition. *Molecules* 22:2267. <https://doi.org/10.3390/molecules22122267>.
- Doi Y, Arakawa Y. 2007. 16S ribosomal RNA methylation: emerging resistance mechanism against aminoglycosides. *Clin Infect Dis* 45:88–94. <https://doi.org/10.1086/518605>.
- Partridge SR, Kwong SM, Firth N, Jensen SO. 2018. Mobile genetic elements associated with antimicrobial resistance. *Clin Microbiol Rev* 31. <https://doi.org/10.1128/CMR.00088-17>.
- Chalmers R, Sewitz S, Lipkow K, Crellin P. 2000. Complete nucleotide sequence of Tn10. *J Bacteriol* 182:2970–2972. <https://doi.org/10.1128/JB.182.10.2970-2972.2000>.
- Peters JE, Craig NL. 2001. Tn7: smarter than we thought. *Nat Rev Mol Cell Biol* 2:806–814. <https://doi.org/10.1038/35099006>.
- Rubens CE, McNeill WF, Farrar WE. 1979. Transposable plasmid deoxyribonucleic acid sequence in *Pseudomonas aeruginosa* which mediates resistance to gentamicin and four other antimicrobial agents. *J Bacteriol* 139:877–882. <https://doi.org/10.1128/jb.139.3.877-882.1979>.
- Partridge SR, Brown HJ, Stokes HW, Hall RM. 2001. Transposons Tn1696 and Tn21 and their integrons In4 and In2 have independent origins. *Antimicrob Agents Chemother* 45:1263–1270. <https://doi.org/10.1128/AAC.45.4.1263-1270.2001>.
- Guo X, Rao Y, Guo L, Xu H, Lv T, Yu X, Chen Y, Liu N, Han H, Zheng B. 2019. Detection and genomic characterization of a *Morganella morgani* isolate from China that produces NDM-5. *Front Microbiol* 10:1156. <https://doi.org/10.3389/fmicb.2019.01156>.
- Rajagopala SV, Casjens S, Uetz P. 2011. The protein interaction map of bacteriophage lambda. *BMC Microbiol* 11:213. <https://doi.org/10.1186/1471-2180-11-213>.
- Roberts AP, Chandler M, Courvalin P, Guédon G, Mullany P, Pembroke T, Rood JI, Smith CJ, Summers AO, Tsuda M, Berg DE. 2008. Revised nomenclature for transposable genetic elements. *Plasmid* 60:167–173. <https://doi.org/10.1016/j.plasmid.2008.08.001>.
- Zhan Z, Hu L, Jiang X, Zeng L, Feng J, Wu W, Chen W, Yang H, Yang W, Gao B, Yin Z, Zhou D. 2018. Plasmid and chromosomal integration of four novel *bla*<sub>IMP</sub>-carrying transposons from *Pseudomonas aeruginosa*, *Klebsiella pneumoniae* and an *Enterobacter* sp. *J Antimicrob Chemother* 73:3005–3015. <https://doi.org/10.1093/jac/dky288>.
- Partridge SR, Hall RM. 2004. Complex multiple antibiotic and mercury resistance region derived from the r-det of NR1 (R100). *Antimicrob Agents Chemother* 48:4250–4255. <https://doi.org/10.1128/AAC.48.11.4250-4255.2004>.
- Alton NK, Vapnek D. 1979. Nucleotide sequence analysis of the chloramphenicol resistance transposon Tn9. *Nature* 282:864–869. <https://doi.org/10.1038/282864a0>.
- Liebert CA, Hall RM, Summers AO. 1999. Transposon Tn21, flagship of the floating genome. *Microbiol Mol Biol Rev* 63:507–522. <https://doi.org/10.1128/MMBR.63.3.507-522.1999>.
- Minnullina L, Pudova D, Shagimardanova E, Shigapova L, Sharipova M, Mardanov A. 2019. Comparative genome analysis of uropathogenic

- strains. *Front Cell Infect Microbiol* 9:167. <https://doi.org/10.3389/fcimb.2019.00167>.
32. Rahman A, Bhuiyan OF, Sadique A, Afroze T, Sarker M, Momen AMI, Alam J, Hossain A, Khan I, Rahman KF, Kamruzzaman M, Shams F, Ahsan GU, Hossain M. 2020. Whole genome sequencing provides genomic insights into three *Morganella morganii* strains isolated from bovine rectal swabs in Dhaka, Bangladesh. *FEMS Microbiol Lett* 367:fnaa043. <https://doi.org/10.1093/femsle/fnaa043>.
  33. Palmieri N, Hess C, Hess M, Alispahic M. 2020. Sequencing of five poultry strains elucidates phylogenetic relationships and divergence in virulence genes in *Morganella morganii*. *BMC Genomics* 21:579. <https://doi.org/10.1186/s12864-020-07001-2>.
  34. Fox GE, Wisotzkey JD, Jurtshuk P, Jr. 1992. How close is close: 16S rRNA sequence identity may not be sufficient to guarantee species identity. *Int J Syst Bacteriol* 42:166–170. <https://doi.org/10.1099/00207713-42-1-166>.
  35. Nelson ML, Levy SB. 2011. The history of the tetracyclines. *Ann N Y Acad Sci* 1241:17–32. <https://doi.org/10.1111/j.1749-6632.2011.06354.x>.
  36. Roberts MC. 2005. Update on acquired tetracycline resistance genes. *FEMS Microbiol Lett* 245:195–203. <https://doi.org/10.1016/j.femsle.2005.02.034>.
  37. Zaric RZ, Jankovic S, Zaric M, Milosavljevic M, Stojadinovic M, Pejicic A. 2021. Antimicrobial treatment of *Morganella morganii* invasive infections: systematic review. *Indian J Med Microbiol*. <https://doi.org/10.1016/j.ijmm.2021.06.005>.
  38. Zhang X, Zou A, Zhang Y, Jianzhong Y, Chuanling M, Zhou T, Cao J. 2014. Prevalence and plasmid characterization of the *qnrD* determinant in *Morganella morganii* isolates. *Chin J Microbiol Immunol* 34:23–28.
  39. Mahrouki S, Perilli M, Bourouis A, Chihi H, Ferjani M, Ben Moussa M, Amicosante G, Belhadj O. 2013. Prevalence of quinolone resistance determinant *qnrA6* among broad-and extended-spectrum beta-lactam-resistant *Proteus mirabilis* and *Morganella morganii* clinical isolates with *sul1*-type class 1 integron association in a Tunisian Hospital. *Scand J Infect Dis* 45:600–605. <https://doi.org/10.3109/00365548.2013.795657>.
  40. Yaiche MN, Raftaf ID, Guo Q, Mastouri M, Aouni M, Wang M. 2014. Type II and type IV topoisomerase mutations in clinical isolates of *Morganella morganii* harbouring the *qnrD* gene. *Ann Clin Microbiol Antimicrob* 13: 34–34. <https://doi.org/10.1186/s12941-014-0034-4>.
  41. Olaitan AO, Diene SM, Gupta SK, Adler A, Assous MV, Rolain J-M. 2014. Genome analysis of NDM-1 producing *Morganella morganii* clinical isolate. *Expert Rev Anti Infect Ther* 12:1297–1305. <https://doi.org/10.1586/14787210.2014.944504>.
  42. Tavio MM, Vila J, Ruiz J, Martín Sánchez AM, Jiménez de Anta MT. 2000. Decreased permeability and enhanced proton-dependent active efflux in the development of resistance to quinolones in *Morganella morganii*. *Int J Antimicrob Agents* 14:157–160. [https://doi.org/10.1016/S0924-8579\(00\)00117-5](https://doi.org/10.1016/S0924-8579(00)00117-5).
  43. Strahilevitz J, Jacoby GA, Hooper DC, Robicsek A. 2009. Plasmid-mediated quinolone resistance: a multifaceted threat. *Clin Microbiol Rev* 22: 664–689. <https://doi.org/10.1128/CMR.00016-09>.
  44. Clinical and Laboratory Standards Institute. 2020. CLSI: performance standards for antimicrobial susceptibility testing, 30th ed. CLSI supplement M100. Clinical and Laboratory Standards Institute, Wayne, PA.
  45. Sun F, Yin Z, Feng J, Qiu Y, Zhang D, Luo W, Yang H, Yang W, Wang J, Chen W, Xia P, Zhou D. 2015. Production of plasmid-encoding NDM-1 in clinical *Raoultella ornithinolytica* and *Leclercia adecarboxylata* from China. *Front Microbiol* 6:458. <https://doi.org/10.3389/fmicb.2015.00458>.
  46. De Coster W, D'Hert S, Schultz DT, Cruts M, Van Broeckhoven C. 2018. NanoPack: visualizing and processing long-read sequencing data. *Bioinformatics* 34:2666–2669. <https://doi.org/10.1093/bioinformatics/bty149>.
  47. Fu J, Zhang J, Yang L, Ding N, Yue L, Zhang X, Lu D, Jia X, Li C, Guo C, Yin Z, Jiang X, Zhao Y, Chen F, Zhou D. 2021. Precision methylome and in vivo methylation kinetics characterization of *Klebsiella pneumoniae*. *Genomics Proteomics Bioinformatics* S1672-0229:00132-7. <https://doi.org/10.1016/j.gpb.2021.04.002>.
  48. Jain C, Rodriguez-R LM, Phillippy AM, Konstantinidis KT, Aluru S. 2018. High throughput ANI analysis of 90K prokaryotic genomes reveals clear species boundaries. *Nat Commun* 9:8. <https://doi.org/10.1038/s41467-018-07641-9>.
  49. Delcher AL, Salzberg SL, Phillippy AM. 2003. Using MUMmer to identify similar regions in large sequence sets. *Curr Protoc Bioinformatics* : 10.3.1–10.3.18. <https://doi.org/10.1002/0471250953.bi1003s00>.
  50. Didelot X, Wilson DJ. 2015. ClonalFrameML: efficient inference of recombination in whole bacterial genomes. *PLoS Comput Biol* 11:e1004041. <https://doi.org/10.1371/journal.pcbi.1004041>.
  51. Stamatakis A. 2006. RAxML-VI-HPC: maximum likelihood-based phylogenetic analyses with thousands of taxa and mixed models. *Bioinformatics* 22:2688–2690. <https://doi.org/10.1093/bioinformatics/btl446>.
  52. Bruun AF. 1950. The systema naturae of the 20th century. *Science* 112: 342–343. <https://doi.org/10.1126/science.112.2908.342-a>.
  53. Luo X, Yin Z, Zeng L, Hu L, Jiang X, Jing Y, Chen F, Wang D, Song Y, Yang H, Zhou D. 2021. Chromosomal integration of huge and complex *bla*<sub>NDM</sub>-carrying genetic elements in Enterobacteriaceae. *Front Cell Infect Microbiol* 11:690799. <https://doi.org/10.3389/fcimb.2021.690799>.
  54. Chen L, Hu H, Chavda KD, Zhao S, Liu R, Liang H, Zhang W, Wang X, Jacobs MR, Bonomo RA, Kreiswirth BN. 2014. Complete sequence of a KPC-producing IncN multidrug-resistant plasmid from an epidemic *Escherichia coli* sequence type 131 strain in China. *Antimicrob Agents Chemother* 58:2422–2425. <https://doi.org/10.1128/AAC.02587-13>.
  55. Wang L, Fung H, Feng J, Yin Z, Xie X, Zhu X, Wang J, Chen W, Yang R, Du H, Zhou D. 2015. Complete sequences of KPC-2-encoding plasmid p628-KPC and CTX-M-55-encoding p628-CTXM coexisted in *Klebsiella pneumoniae*. *Front Microbiol* 6:838. <https://doi.org/10.3389/fmicb.2015.00838>.
  56. Yu T, Yang H, Li J, Chen F, Hu L, Jing Y, Luo X, Yin Z, Zou M, Zhou D. 2021. Novel chromosome-borne accessory genetic elements carrying multiple antibiotic resistance genes in *Pseudomonas aeruginosa*. *Front Cell Infect Microbiol* 11:638087. <https://doi.org/10.3389/fcimb.2021.638087>.
  57. Partridge SR, Ginn AN, Paulsen IT, Iredell JR. 2012. pEI1573 carrying *bla*<sub>IMP-4/7</sub> from Sydney, Australia, is closely related to other IncL/M plasmids. *Antimicrob Agents Chemother* 56:6029–6032. <https://doi.org/10.1128/AAC.01189-12>.
  58. Heffron F, Sublett R, Hedges R, Jacob A, Falkow S. 1975. Origin of the TEM-beta-lactamase gene found on plasmids. *J Bacteriol* 122:250–256. <https://doi.org/10.1128/jb.122.1.250-256.1975>.
  59. Feng J, Qiu Y, Yin Z, Chen W, Yang H, Yang W, Wang J, Gao Y, Zhou D. 2015. Coexistence of a novel KPC-2-encoding MDR plasmid and an NDM-1-encoding pNDM-HN380-like plasmid in a clinical isolate of *Citrobacter freundii*. *J Antimicrob Chemother* 70:2987–2991. <https://doi.org/10.1093/jac/dkv232>.
  60. Liu J, Keelan P, Bennett PM, Enne VI. 2009. Characterization of a novel macrolide efflux gene, *mef(B)*, found linked to *sul3* in porcine *Escherichia coli*. *J Antimicrob Chemother* 63:423–426. <https://doi.org/10.1093/jac/dkn523>.
  61. Golebiewski M, Kern-Zdanowicz I, Zienkiewicz M, Adamczyk M, Zylinska J, Baraniak A, Gniadkowski M, Bardowski J, Ceglowski P. 2007. Complete nucleotide sequence of the pCTX-M3 plasmid and its involvement in spread of the extended-spectrum beta-lactamase gene *bla*<sub>CTX-M-3</sub>. *Antimicrob Agents Chemother* 51:3789–3795. <https://doi.org/10.1128/AAC.00457-07>.
  62. Wrighton CJ, Strike P. 1987. A pathway for the evolution of the plasmid NTP16 involving the novel kanamycin resistance transposon Tn4352. *Plasmid* 17:37–45. [https://doi.org/10.1016/0147-619x\(87\)90006-0](https://doi.org/10.1016/0147-619x(87)90006-0).
  63. L'Abée-Lund TM, Sørnum H. 2000. Functional Tn5393-like transposon in the R plasmid pRAS2 from the fish pathogen *Aeromonas salmonicida* subspecies *salmonicida* isolated in Norway. *Appl Environ Microbiol* 66: 5533–5535. <https://doi.org/10.1128/AEM.66.12.5533-5535.2000>.